https://doi.org/10.5194/egusphere-2026-3669
Preprint. Discussion started: 23 September 2026

Intra-seasonal flow variability and a probable long-term slowdown of Universidad Glacier in the Central Andes of Chile (34° S)

Christopher Ulloa[1,2], Ayon García[1,2], Hans Fernández-Navarro[3], Jorge Berkhoff[4], José Luis Rodriguez[3,5], Pierre Pitte[6].

1 LICA-DICTEC/Laboratorio de investigación de la criósfera y aguas, Universidad de Atacama (1530000), Avenida Copayapu #485, Copiapó, Chile.
2 Departamento de geología Universidad de Atacama. (1530000), Avenida Copayapu #485, Copiapó, Chile.
3 Instituto de Ciencias Agroalimentarias, Animales y Ambientales (ICA3), Universidad de O'Higgins (2820000), San Fernando, Chile.
4 Institut für Geographie, Friedrich-Alexander-Universität Erlangen-Nürnberg, Erlangen, Germany.
5 Instituto de ciencias físicas y matemáticas, facultad de ciencias, Universidad Austral de Chile (5110566), Valdivia, Chile.
6 Instituto Argentino de Nivología, Glaciología y Ciencias Ambientales (IANIGLA), Universidad Nacional de Cuyo, CONICET (5500), Ruiz Leal S/N, Parque General San Martín, Mendoza, Argentina.

Correspondence to: Christopher Ulloa (christopher.ulloa@uda.cl)

Abstract. Understanding glacier dynamics in semiarid mountain regions is essential for assessing water availability and anticipating the impacts of climate variability. Here, we present the first characterization of surface velocity dynamics at Universidad Glacier, a 24.91 km² valley glacier in the semiarid Central Andes of Chile, using Sentinel-1 SAR offset tracking during two consecutive ablation seasons (2023–2024 and 2024–2025), compared with in situ GNSS stake measurements. Multi-temporal velocity fields and along-centerline profiles reveal a stable spatial flow structure: velocities peak in the mid-glacier icefall zone (3,000–3,500 m a.s.l.; up to 0.3–0.6 m d⁻¹ in individual 12-day fields, and 0.16 and 0.08 m d⁻¹ as season means in 2023–2024 and 2024–2025, respectively) and decrease both upstream, where values are indistinguishable from the off-glacier noise level (~0.10 m d⁻¹), and downstream along the debris-covered lower tongue. Superimposed on this structure, the icefall velocity in the January–February pairs of both seasons (0.03–0.06 m d⁻¹) is at the stable-terrain noise floor, whereas the March pairs show a clear increase (to 0.10 and 0.06 m d⁻¹; 2–4 times the noise level). The higher December 2023 values and the April values of both seasons coincide with elevated velocities across the entire glacier, including the accumulation area, and cannot yet be separated from decorrelation artifacts. A first-order comparison with in situ and ERA5-Land air temperature shows that total thermal forcing was nearly identical between seasons and that velocity was not in phase with air temperature: in 2024–2025 the March increase followed the seasonal temperature maximum by 4–5 weeks. A lagged subglacial-drainage response is discussed as a working hypothesis alongside methodological alternatives. Comparison with GNSS stakes (n = 11; RMSE = 0.022 m d⁻¹, bias = −0.011 m d⁻¹, regression slope = 0.51) indicates good agreement in the spatial ranking of velocities but systematic underestimation of the fastest stake, over a validated range of 0.01–0.16 m d⁻¹. Season-mean velocities are 4–8 times lower than the ITS_LIVE 1986–2025 median and 2–4 times lower

https://doi.org/10.5194/egusphere-2026-3669
Preprint. Discussion started: 23 September 2026

than the ITS_LIVE 2020–2025 median; because a factor of 2–4 is attributable to the spatial smoothing of our offset-tracking configuration, the multidecadal deceleration is considered likely but not yet quantified. These results establish a high-temporal-resolution velocity baseline for Universidad Glacier and identify the processing and observational requirements needed to detect melt-driven dynamic variability that multi-annual velocity products cannot resolve.

1 Introduction

Glaciers in semiarid mountain regions are essential components of local hydrological systems, providing critical water resources during dry seasons when precipitation is scarce (Vuille et al., 2008; Masiokas et al., 2020). In the Central Andes of Chile and Argentina, glacier sizes span a wide range according to national and global inventories. While many glaciers are small, a number of mid-sized and large valley glaciers are associated with major massifs such as Tupungato (6,570 m a.s.l.) and Picos de Barroso (5,171 m a.s.l.), binational peaks along the Chile–Argentina border. Based on the Randolph Glacier Inventory (RGI v6.0), the global mean individual glacier area is approximately 0.62 km^2, with a large standard deviation of ~2.3 km^2, reflecting a strongly right-skewed size distribution dominated numerically by small glaciers but including a limited number of much larger ice bodies. Universidad Glacier, with an area of 24.91 km^2, is the largest valley glacier in the Chilean Central Andes. Despite their larger size, such glaciers can still exhibit pronounced seasonal and sub-seasonal velocity variability, making them well suited for evaluating how global velocity products represent melt-driven dynamics (Millan et al., 2022; Strozzi et al., 2002).

Glacier dynamics, particularly surface velocities, provide key insights into ice flow, stress balance, and the response of glaciers to climate variability (Cuffey & Paterson, 2010). Continuous measurements of ice motion are critical for understanding mass redistribution, detecting instabilities, and constraining numerical models of ice thickness and volume (Farinotti et al., 2019; Zemp et al., 2019). However, in the Central Andes, in situ measurements remain scarce due to difficult access, harsh conditions, and limited logistical support. As a result, most assessments rely on satellite remote sensing, which has emerged as the primary tool to investigate glacier evolution in this region (Kääb et al., 2016; Hugonnet et al., 2021).

In recent years, a complementary effort has been initiated to establish detailed in situ monitoring networks on selected glaciers in central Chile. On Universidad Glacier, an array of ablation stakes was installed during the 2024 field campaign (Fig. 1). These stakes represent the first intensive monitoring program of this glacier, led by the Instituto de Ciencias Agroalimentarias, Animales y Ambientales of Universidad de O'Higgins (ICA3-UOH) in collaboration with the Chilean Ministry of Public Works (Dirección General de Aguas, MOP-DGA). The stake network provides high-resolution, ground-based observations of ice melt and flow, which are essential for validating satellite-derived velocity fields and for improving our understanding of glacier response to climate variability in semiarid mountain environments.

Synthetic Aperture Radar (SAR) imagery, and particularly the Sentinel-1 constellation, has transformed the monitoring of glacier surface velocities. Offset tracking techniques applied to SAR data enable robust measurements of glacier flow under

https://doi.org/10.5194/egusphere-2026-3669
Preprint. Discussion started: 23 September 2026

all-weather and day–night conditions, overcoming the limitations of optical imagery in cloud-prone or seasonally snow-covered areas (Strozzi et al., 2002; Nagler et al., 2015; Paul et al., 2017). Recent studies have demonstrated the potential of Sentinel-1 time series to capture seasonal velocity fluctuations, short-term accelerations, and long-term trends in diverse glaciated regions (Millan et al., 2022; Falaschi et al., 2019; Sánchez-Gámez and Navarro, 2017). However, while global velocity products provide robust representations of long-term flow regimes, their ability to resolve seasonal and sub-seasonal dynamics in large valley glaciers remains limited, and such short-term glacier dynamics are still poorly documented.

This study presents the first characterization of surface velocity dynamics at Universidad Glacier, located in the Central Andes of Chile. Using Sentinel-1 SAR offset tracking over two consecutive ablation seasons (2023–2024 and 2024–2025), compared with in situ GNSS measurements, we pursue three specific objectives: (1) establish a high-temporal-resolution velocity baseline for this previously undocumented glacier; (2) identify and characterize intra-seasonal velocity fluctuations and their spatial patterns; and (3) evaluate how global and multi-annual velocity products (ITS_LIVE, Millan et al., 2022) represent or fail to represent these short-term dynamics. The results contribute a first observational foundation for future multi-year monitoring and hydrological studies at Universidad Glacier, and provide a case study illustrating the limitations of global velocity climatologies for resolving melt-driven dynamics in semiarid Andean glaciers.

https://doi.org/10.5194/egusphere-2026-3669
Preprint. Discussion started: 23 September 2026

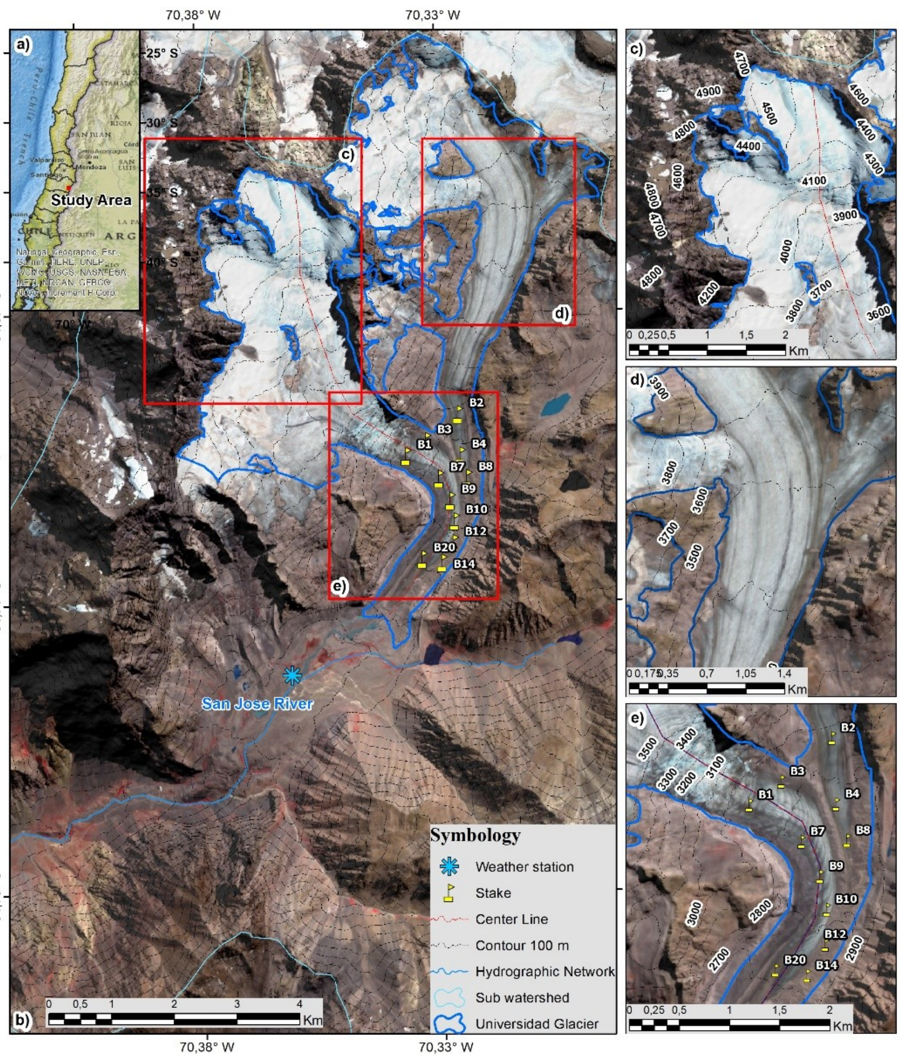

Figure 1. Universidad Glacier location and stake distribution during the 2024-2025 field campaign. Panel (a) shows the study area location. Panel (b) presents the glacier outline, centerline, contour lines, and stake distribution. Panels (c) and (d) show detailed views of the upper glacier sectors, while panel (e) shows the stake network in the lower ablation zone, where the highest stake density was concentrated. The 2025 glacier outline is shown in blue (Sentinel-2 imagery from 12 March 2025).

2 Study area

Universidad Glacier is located on the southern edge of the Central Andes of Chile, in the mountain range of the O'Higgins Region (Fig. 1). The climate regime of the area is characterized by warm and dry summers (December–March), associated with the strengthening and southward displacement of the Pacific Subtropical Anticyclone (Flores-Aqueveque et al., 2020; Garreaud, 2009). In contrast, low temperatures and winter precipitation (May–September) are linked to the seasonal northward migration of the Westerly Winds, a sub-Antarctic belt of low-pressure systems (Garreaud, 2009). The interannual

https://doi.org/10.5194/egusphere-2026-3669
Preprint. Discussion started: 23 September 2026

variability of the latitudinal position of the Westerly Winds has been associated with the El Niño–Southern Oscillation (ENSO) phenomenon (Garreaud, 2009; Montecinos & Aceituno, 2003) and with the Southern Annular Mode (SAM) (Garreaud et al., 2020).

The mountain range in the O'Higgins Region lacks meteorological data collected systematically over the long term. The nearest weather station with a long-term continuous record is located 117 km to the north, in the mountains near Santiago, the capital of Chile. Shorter records exist closer to the glacier: an automatic weather station operated on the glacier during 2012–2014 (Kinnard et al., 2018), and DGA station 06023000-5, ~5 km from the glacier margin, has operated intermittently since November 2022 (Sect. 3.5). According to climate data from the El Embalse El Yeso station (33° 40' S – 70° 5' W), the average annual temperature at 2,400 m a.s.l. is 8.3°C, and the average annual precipitation reaches 515 mm (Barcaza et al., 2017). The Equilibrium Line Altitude (ELA) in the Universidad Glacier area fluctuated between 3,480 m a.s.l. and 4,230 m a.s.l. during the 2012/13 and 2013/14 periods, respectively (Kinnard et al., 2018). For the 2024/25 period, the ELA remained at 3,700 m a.s.l. (DGA and UOH, 2026).

Universidad Glacier covers 24.91 km², and its tongue, fed mainly by two cirques, extends southward for approximately 10 km. The glacier is surrounded by high peaks reaching ~5,000 m a.s.l. To the west, prominent peaks include Cerro Alto Los Arrieros (4,990 m a.s.l.) and Cerro El Portillo (4,960 m a.s.l.), which are part of the "Sierra del Brujo" mountain range. To the north stands the El Palomo volcano (4,860 m a.s.l.), which has no reports of recent volcanic activity. The highest sections of the glacier reach approximately 4,540 m a.s.l., while its front descends to 2,500 m a.s.l. (Fernández-Navarro et al., 2023). Between 3,500 and 3,000 m a.s.l., a pronounced topographic step produces a heavily crevassed area. The lower glacier tongue is characterized by debris cover derived from the medial moraine, the collapse of lateral moraines, and glaciotectonic activity (Fernández et al., 2022). The development of this debris cover has been linked to decreasing precipitation and rising air temperatures in recent decades (Podgórski et al., 2023), as well as to abrupt changes in glacier velocity and the subsequent emergence of subglacial debris (Fernández et al., 2022).

To clearly differentiate the glacier sectors discussed in this study, we hereafter refer to elevations above 3,500 m a.s.l. as the upper zone, those between 3,500 and 3,000 m a.s.l. as the mid-zone, and those below 3,000 m a.s.l. as the lower zone (Fig. 1). The velocity maximum described in Sect. 4 lies within the mid-zone, at the icefall; we use "icefall zone" for this sector and "lower tongue" for the lower zone, and reserve "tongue" for the ablation area below the icefall as a whole.

3 Methodology

3.1 Satellite data and offset tracking

We applied SNAP v9.0 offset tracking to Sentinel-1 IW GRD pairs, following DEM-assisted co-registration (SRTM 30 m). Displacement was retrieved with a 128×128 pixel window (~1.3 km on the ground, comparable to the tongue width, so that icefall maxima are attenuated; Sect. 4.3) at 200 m grid spacing, converted to m d^{-1}. The 36-day 10 Feb–18 Mar 2025 pair

https://doi.org/10.5194/egusphere-2026-3669
Preprint. Discussion started: 23 September 2026

yielded two independent solutions (v1, v2), both with an icefall signal at the noise level (Table S1); it is excluded from the quantitative analyses (Sect. 4.1, 4.6) though listed in Table 2 and deposited with the data.

A directional post-processing filter, combined with an outline mask, was applied only to the illustrative vector-field figures (Fig. 6, S4) to suppress false-positive orientations in the low-velocity upper glacier; full methodological detail is given in the Supplement (Sect. S1). Unless otherwise stated, all statistics and profiles reported here (Figs. 2–6, 8–9; Tables 2–3) use the raw, unfiltered magnitude rasters. The processing workflow is summarised in Fig. S3.

3.2 Glacier centerline and zonation

A glacier centerline was manually digitized from a 2025 Landsat-9 image and used to extract along-flow velocity information. The centerline was subdivided into upper, mid, and lower glacier zones based on DEM-derived hypsometry. For each Sentinel-1 image pair, velocity magnitudes were first obtained from the offset-tracking raster products and then interpolated at the vertices of the centerline polyline to ensure consistent spatial sampling along the flowline. This procedure allowed the construction of time-series profiles for each season. To minimize local noise while retaining intra-seasonal variability, the extracted velocity series were smoothed using a LOWESS regression (fraction = 0.45), providing robust velocity profiles for inter- and intra-seasonal comparison. Uncertainty bars shown in the along-centerline profiles (Figs. 2 and 6) represent two distinct quantities that are not directly comparable to the theoretical tracking uncertainty. In Fig. 2, bars show the spatial standard deviation of velocity within a 200 m buffer around each centerline vertex (typically 0.01–0.02 m d^{-1}), reflecting local spatial heterogeneity rather than instrumental precision; in Fig. 6, bars show the standard deviation of the season-mean velocity across image pairs, reflecting intra-seasonal temporal variability. Neither quantity includes the theoretical tracking uncertainty (0.05–0.08 m d^{-1}, Sect. 3.4), which is substantially larger than both and represents a separate, dominant source of uncertainty that should be considered independently, not combined with the plotted bars, when assessing the absolute reliability of any individual value.

3.3 GNSS stake network and field observations

To validate the remote sensing results, we installed a network of eleven GNSS stakes across the lower zone of Universidad Glacier (Fig. 1e), to capture the spatial variability in ice flow dynamics. Each stake was monitored with dual-frequency GNSS receivers operating in static mode. Data were differentially corrected against a nearby reference station, yielding sub-decimeter positioning accuracy. Each stake was surveyed twice, at the start (06 April 2024) and end (28 April 2025) of the monitoring period; velocities were computed as the horizontal displacement between these two surveys divided by the elapsed time (≈387 days) and expressed in meters per day. These values therefore represent an annual mean velocity spanning both ablation seasons and the intervening winter, rather than measurements coeval with individual Sentinel-1 pairs.

Table 1 Geographic coordinates of the ablation stakes installed on Universidad Glacier in April 2024 and surveyed during the 2024–2025 mass balance campaign, with the GNSS survey interval used for comparison with Sentinel-1.

https://doi.org/10.5194/egusphere-2026-3669
Preprint. Discussion started: 23 September 2026

Stake ID	Latitude (°)	Longitude (°)	Begin GNSS date	End GNSS date
B1	-34.687425	-70.338907	2024-04-06	2025-04-28
B2	-34.681513	-70.329825	2024-04-06	2025-04-28
B3	-34.685353	-70.335410	2024-04-06	2025-04-28
B4	-34.687461	-70.329463	2024-04-06	2025-04-28
B7	-34.690764	-70.333275	2024-04-06	2025-04-28
B8	-34.690713	-70.328350	2024-04-06	2025-04-28
B9	-34.693908	-70.331330	2024-04-06	2025-04-28
B10	-34.696884	-70.330649	2024-04-06	2025-04-28
B12	-34.700058	-70.330847	2024-04-06	2025-04-28
B14	-34.702821	-70.332879	2024-04-06	2025-04-28
B20	-34.702277	-70.336308	2024-04-06	2025-04-28

3.4 Uncertainty assessment

Uncertainty in SAR-derived velocities arises from both image matching and geometric configuration. Based on our offset-tracking setup (window size 128 px, oversampling factor 16, and grid spacing of 200 m), the theoretical sub-pixel precision of displacement estimates is on the order of ~0.05–0.08 pixels. We note that the oversampling factor sets the quantization step of the offset estimate (1/16 = 0.0625 px), whereas the matching precision reported for glacier surfaces is typically 0.1–0.2 px (Strozzi et al., 2002; Joughin, 2002; Sánchez-Gámez and Navarro, 2017); the value adopted here is therefore an optimistic bound. For the 12-day pairs and the 10 m GRD pixel spacing this corresponds to approximately ~0.05–0.08 m d^{-1}; for the 24- and 36-day pairs the equivalent bound scales inversely with the baseline (~0.03–0.04 and ~0.02–0.03 m d^{-1}, respectively), although the longer pairs are more affected by temporal decorrelation. This was compared empirically with GNSS stakes (n = 11), which yielded RMSE = 0.022 m d^{-1} and BIAS = −0.011 m d^{-1} over a velocity range of 0.01–0.16 m d^{-1}, with a regression slope of 0.51 (Sect. 4.3). The lower RMSE relative to the theoretical bound is consistent with the fact that the GNSS stakes are located in the mid- to lower glacier, where surface coherence is relatively high and image correlation is more reliable; the theoretical estimate encompasses the full range of conditions including crevassed and debris-covered zones where uncertainty is higher. The empirical RMSE should therefore be regarded as a lower-bound estimate, applicable primarily to coherent, moderate-velocity areas, while the theoretical range better represents the worst-case uncertainty across the full glacier surface. Additional uncertainty sources include temporal decorrelation in steep or crevassed areas and noise in debris-covered surfaces; these effects were minimized through DEM-assisted co-registration, averaging in a 5 × 5 moving window, and profile-scale smoothing. For clarity, the three uncertainty estimates used throughout this study are summarised here with their derivation and scope of applicability: (1) theoretical sub-pixel bound (0.05–0.08 m d^{-1}), representing worst-case uncertainty across the full glacier surface including crevassed and debris-covered zones; (2) empirical off-glacier detection threshold (~0.10 m d^{-1}, P90 of stable-terrain pixels), defining the minimum detectable glacier velocity; and (3) empirical GNSS validation RMSE (0.022 m d^{-1}), representing a lower-bound estimate

https://doi.org/10.5194/egusphere-2026-3669
Preprint. Discussion started: 23 September 2026

applicable to coherent, slow-moving areas (0.01–0.16 m d⁻¹) of the lower glacier; the velocity range in which the intra-seasonal changes discussed in Sect. 4–5 occur (0.2–0.5 m d⁻¹, icefall zone) is not sampled by the stake network. Throughout the paper, velocity differences smaller than the detection threshold (2) are reported but not interpreted as dynamic signals.

Image pairs were selected to maximize temporal continuity during the ablation seasons of 2023–2024 and 2024–2025, while ensuring adequate coherence over the glacier surface. All acquisitions correspond to ascending orbits, which provide consistent viewing geometry across both study years. The selected pairs span December to April, with temporal baselines ranging from 12 to 36 days, thus capturing both short-term and extended intervals of glacier motion. A complete list of the Sentinel-1 image pairs used in this study, including acquisition dates, temporal baselines, and orbit direction, is provided in Table 2. These datasets form the basis for offset-tracking analysis and subsequent construction of multi-temporal velocity fields and along-flow profiles.

Table 2 Sentinel-1 GRD image pairs (ascending orbits) used for offset tracking at Universidad Glacier during the 2023–2024 and 2024–2025 ablation seasons.

Season	Acquisition pair (start–end)	Baseline (days)	Off-glac. P90 (m d⁻¹)	Orbit direction	Notes
2023–2024	06–18 Dec 2023	12	0.089	Ascending	Early summer, good coherence
	18–30 Dec 2023	12	0.097	Ascending	—
	11–23 Jan 2024	12	0.081	Ascending	—
	04–16 Feb 2024	12	0.056	Ascending	—
	16–28 Feb 2024	12	0.072	Ascending	—
	11–23 Mar 2024	12	0.087	Ascending	—
	04–16 Apr 2024	12	0.130	Ascending	Late season
2024–2025	12–24 Dec 2024	12	0.061	Ascending	Early summer
	12 Dec 2024 – 05 Jan 2025	24	0.077	Ascending	Long baseline
	05–17 Jan 2025	12	0.079	Ascending	—
	29 Jan – 10 Feb 2025	12	0.069	Ascending	—
	10 Feb – 18 Mar 2025	36	0.022	Ascending	Extended interval; excluded from quantitative analyses (Table S1; Sect. 3.1)
	06–18 Mar 2025	12	0.057	Ascending	—
	11–23 Apr 2025	12	0.151	Ascending	Late season

https://doi.org/10.5194/egusphere-2026-3669
Preprint. Discussion started: 23 September 2026

3.5 Air temperature data: ERA5-Land and in situ station

To provide first-order hydrometeorological context for the intra-seasonal velocity fluctuations (Sect. 4.6), we extracted ERA5-Land hourly 2 m air temperature (Muñoz-Sabater et al., 2021) averaged over the glacier catchment for the full duration of both ablation seasons. Daily means were computed and aggregated into cumulative positive degree-days (PDD), used here as a first-order proxy for surface meltwater production, and matched to the exact temporal windows of each Sentinel-1 image pair (Sect. 4.6).

In addition, we obtained hourly meteorological data from DGA station 06023000-5 ("Glaciar Universidad", satellite telemetry, Glaciares-Meteorológicas network; DGA, 2026), located approximately 5 km from the glacier margin (UTM 375541 E, 6157306 N, WGS84 19S). This station provides air temperature, wind, snow depth and accumulated precipitation at native ~1-hour resolution, and, being an in-situ point measurement close to the glacier rather than a coarse-grid reanalysis product, offers a substantially stronger basis for hydrometeorological interpretation than ERA5-Land alone. The station record is intermittent: it was offline from October to December 2023 and from April to June 2024, but otherwise provides near-complete hourly coverage from November 2022 onward, including essentially the entire 2024–2025 ablation season (90–100% of hours per Sentinel-1 pair window, after deduplicating the raw hourly file by timestamp) and the January–March portion of the 2023–2024 season (40–91% coverage per pair window). Where the station has no data (the two December 2023 pairs and the 04–16 April 2024 pair), we retain the ERA5-Land estimate as a fallback. The agreement between the two sources and the temperature conditions of each Sentinel-1 pair window are presented in Sect. 4.6. For basin-scale hydrological context (Sect. 5.5), discharge records for the gauge Río Tinguiririca bajo Los Briones (BNA 06028001-0, ~46 km downstream of the glacier) were obtained from the same DGA platform (DGA, 2026); processing details and the diurnal-amplitude metric are given in the captions of Supplement Figs. S1–S2.

4 Results

4.1 Distribution of surface velocities on the Universidad Glacier

Surface velocity fields of Universidad Glacier, derived from Sentinel-1 offset tracking, reveal marked spatial and temporal variability between the 2023–2024 and 2024–2025 ablation seasons (Figs. 2–4). In both periods, velocities were highest in the mid-glacier icefall zone (3,000–3,500 m a.s.l., DEM-derived; 3.41 km^2), where the tributary cirques converge, and decreased both upstream into the accumulation area and downstream along the narrow lower tongue. We report three distinct quantities, computed from the raw, unfiltered offset-tracking magnitude rasters over the DEM/outline-verified glacier mask (24.92 km^2), which are not interchangeable: (i) the glacier-wide arithmetic mean, averaged first over all on-glacier pixels within each pair and then over the season's pairs, was 0.131 m d^{-1} in 2023–2024 and 0.086 m d^{-1} in 2024–2025; (ii) the on-

https://doi.org/10.5194/egusphere-2026-3669
Preprint. Discussion started: 23 September 2026

glacier median pooled across all pairs of each season, reported in Fig. 8, was 0.094 m d^{-1} and 0.060 m d^{-1} respectively, lower than the mean, as expected for a right-skewed distribution dominated by the slow upper accumulation area (below 0.10 m d^{-1}, i.e. below the detection threshold defined in Sect. 4.4, over most of this zone); and (iii) the icefall-zone mean during each season's fastest pair (04–16 April 2024 and 11–23 April 2025, both discussed further in Sect. 4.2 and 5.2) was 0.245 m d^{-1} and 0.211 m d^{-1}. It should be noted that the difference in glacier-wide mean velocities between seasons (0.045 m d^{-1}) is smaller than the theoretical uncertainty of the method (~0.05–0.08 m d^{-1}), and should therefore not be interpreted as a statistically robust interannual signal at the glacier-wide scale. The same criterion is applied throughout this section: differences smaller than the empirical detection threshold (~0.10 m d^{-1}, Sect. 4.4) are reported but not interpreted as dynamic signals.

Centerline velocity profiles emphasize these contrasts along the longitudinal axis (Fig. 2), sampled at 100 m intervals along the digitized centerline and LOWESS-smoothed (fraction = 0.45) as in Sect. 3.2. In individual 12-day fields the icefall zone (3–5 km from the head) exceeded 0.40 m d^{-1} only during the 04–16 April 2024 pair (0.56 m d^{-1}) and reached 0.31 m d^{-1} during the 11–23 April 2025 pair; during December–March, icefall-zone maxima ranged between 0.05 and 0.18 m d^{-1} in 2023–2024 and between 0.02 and 0.09 m d^{-1} in 2024–2025. The lower tongue (>6.5 km) and the upper zone (0–1.5 km) remained largely below 0.10 m d^{-1} across both periods, with three exceptions: the December 2023 pairs, which show 0.26–0.32 m d^{-1} at the head of the centerline and high values over the north-eastern accumulation cirque (Fig. 3); the 11–23 April 2025 pair, which shows 0.24 m d^{-1} at the head; and the same April 2025 pair, whose lower tongue also reaches 0.17 m d^{-1}, above the detection threshold. Because the upper-glacier values occur over snow-covered, low-contrast surfaces at the start and end of the ablation season and are not reproduced in adjacent pairs, we consider them likely decorrelation artifacts rather than ice motion; the April 2025 tongue value coincides with the same pair already flagged as uncertain in Sect. 4.1 and 5.2. Averaged over the season, mean icefall-and-tongue velocities (centerline points beyond 3 km) were 37.5% lower in 2024–2025 (0.063 m d^{-1}) than in 2023–2024 (0.100 m d^{-1}), a larger contrast than the glacier-wide comparison in Sect. 4.1 because it excludes the near-stagnant upper accumulation area common to both seasons.

Seasonal changes within each ablation period are summarised by the mean velocity of the icefall and tongue (centerline points beyond 3 km; Fig. 9), computed from the same digitized centerline and LOWESS smoothing used in Sect. 4.2. In 2023–2024 this mean is highest in the first pair (06–18 December, 0.120 m d^{-1}), declines through January (0.064) to 0.032 m d^{-1} in the 04–16 February pair, and rises again in March (0.098) and April (0.255). In 2024–2025 the 12-day pairs from December to early February are flat within noise (0.034, 0.031 and 0.034 m d^{-1} for 12–24 December, 05–17 January and 29 January–10 February; the 24-day 12 December–05 January pair gives 0.057), followed by the same March (0.062) and April (0.210) increases. The glacier-wide mean (all on-glacier pixels) shows the same ordering with smaller amplitude: in 2023–2024 it decreased from 0.14 m d^{-1} in December–January to 0.12 m d^{-1} in the 11–23 March pair, a difference within the theoretical uncertainty. Two groups of pairs require caution before any of these changes is interpreted as ice dynamics. First, in every December–February pair of both seasons the icefall values are at or below the stable-terrain noise level (icefall/noise ratios of 0.8–1.2, Table S1), so that neither the flat 2024–2025 sequence nor the magnitude of the 2023–2024

https://doi.org/10.5194/egusphere-2026-3669
Preprint. Discussion started: 23 September 2026

decline can be resolved; only the March pairs (ratios 2.7 and 4.4) and the April pairs (4.8 and 2.7) stand clearly above the noise. Second, the two December 2023 pairs and the April pairs of both seasons show elevated velocities over the entire glacier, including the accumulation area (upper-zone means of 0.24, 0.24, 0.17 and 0.23 m d⁻¹ at 0–1.5 km, exceeding or approaching the icefall mean of the same pair), and coincide with the snow-covered start and the coldest end of the season, when loss of coherence is most likely. A within-glacier criterion makes this explicit: the ratio of the icefall mean (3–5 km) to the upper-zone mean (0–1.5 km) is below 1 in all December–February pairs (0.35–0.87) and above 1 only in March and April (1.4 and 2.8 in 2024; 2.3 and 1.2 in 2025). We therefore treat the two December 2023 pairs and both April pairs as unconfirmed pending pair-specific quality screening (coherence and snow-cover), applying the same criterion to both seasons. The robust intra-seasonal result common to both seasons is a March increase, from noise-level values in January–February to 0.06–0.10 m d⁻¹ in the icefall/tongue mean (0.09–0.14 m d⁻¹ at the icefall maximum).

A pixel-wise comparison of season-mean velocities (Fig. S9, Supplement) shows that the largest interannual decrease (down to −0.25 m d⁻¹) occurs in the upper/western tributary cirque; icefall and lower-tongue differences range from −0.13 to +0.04 m d⁻¹ (mean −0.02 m d⁻¹), while the upper zone as a whole ranges from −0.25 to +0.10 m d⁻¹ (mean −0.05 m d⁻¹). No localized positive anomaly exceeds +0.10 m d⁻¹. Because the strongest decrease is located where the December 2023 pairs show their anomalously high values, it is most likely dominated by those pairs rather than by a dynamic change. Overall, the difference map shows a broadly glacier-wide decrease in 2024–2025 relative to 2023–2024, strongest in the upper/western cirque and weaker over the icefall and tongue.

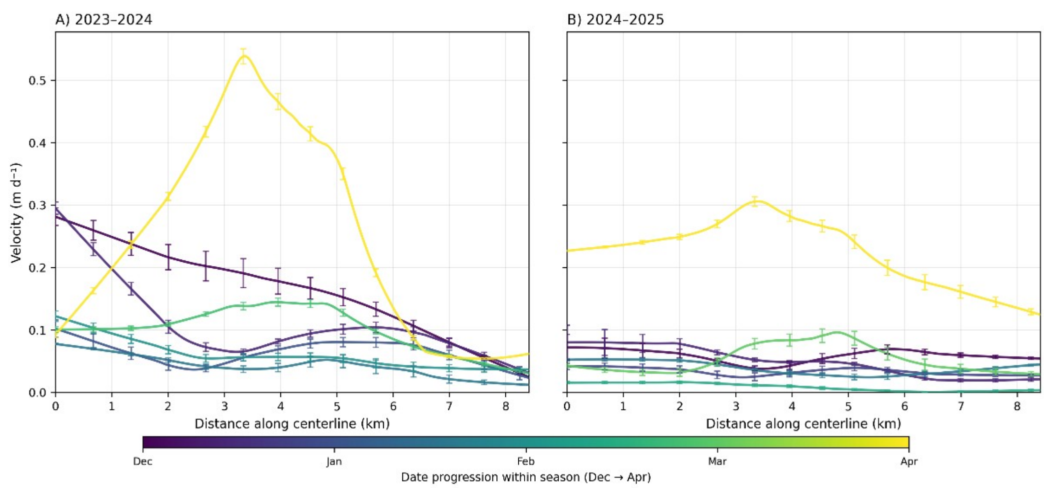

Figure 2. Along-centerline velocity profiles of Universidad Glacier for the ablation seasons A) 2023–2024 and B) 2024–2025, derived from Sentinel-1 offset tracking. Colors indicate the temporal progression from December to April (unified color scale across both seasons). Curves represent smoothed profiles (LOWESS) showing seasonal evolution of ice flow along the glacier centerline.

https://doi.org/10.5194/egusphere-2026-3669
Preprint. Discussion started: 23 September 2026

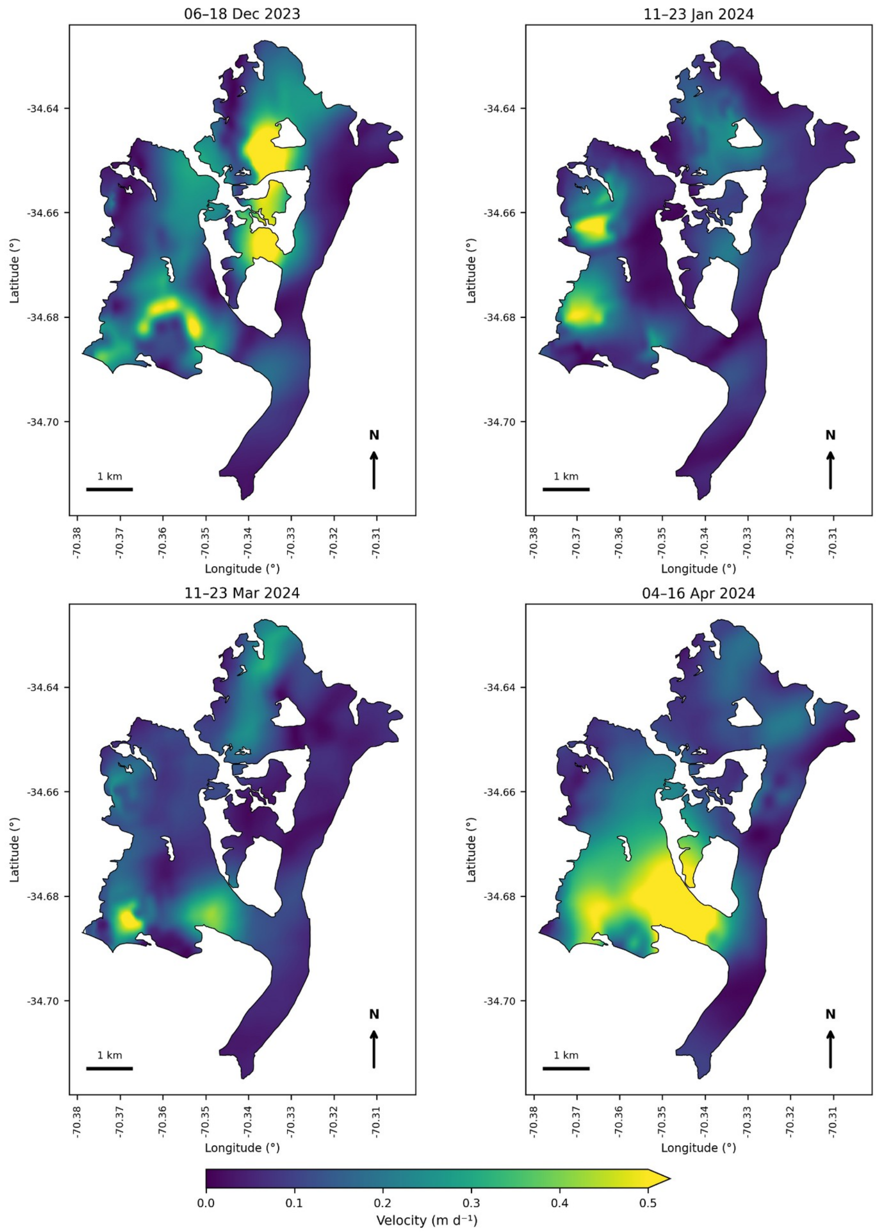

Figure 3. Spatial distribution of surface velocities at Universidad Glacier derived from Sentinel-1 offset tracking for the 2023–2024 ablation season. Four of the seven 12-day pairs (Table 2) are shown (all pairs in Fig. S7), illustrating the temporal evolution from December 2023 to April 2024. Colors indicate ice flow velocity magnitude (m d^{-1}). The 04–16 April 2024 pair is flagged as a probable decorrelation artifact (Sect. 4.1). The arrows indicate north, and the scale bar corresponds to 1 km.

https://doi.org/10.5194/egusphere-2026-3669
Preprint. Discussion started: 23 September 2026

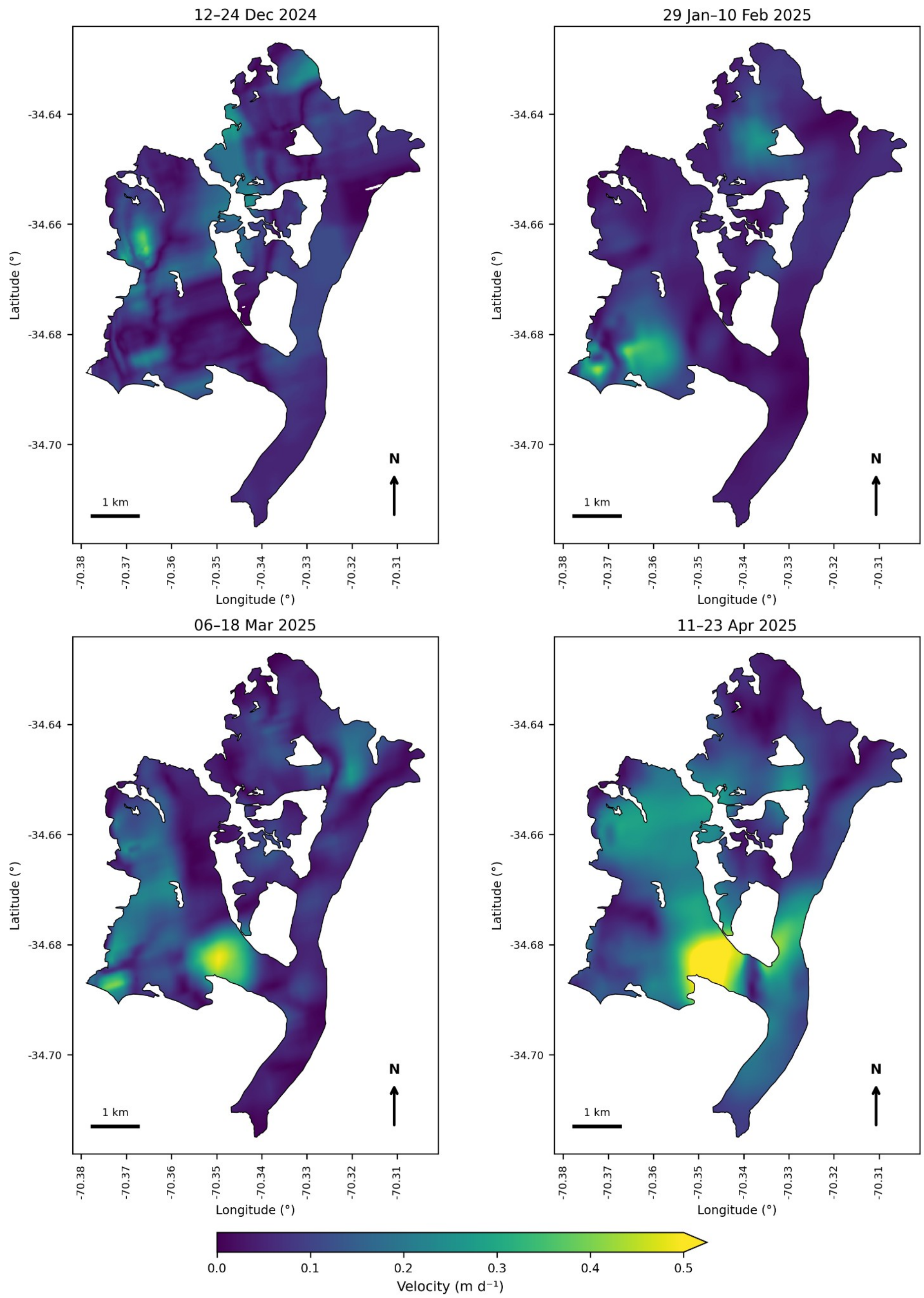

Figure 4. Surface velocity fields of Universidad Glacier during the 2024–2025 ablation season, derived from Sentinel-1 offset tracking. Four of the seven pairs (Table 2) are shown (all pairs in Fig. S8), illustrating the temporal evolution of glacier flow from December 2024 to April 2025. Colors indicate velocity magnitude (m d^{-1}). Note the glacier-wide increase in the 11–23 April 2025 pair, discussed in Sect. 4.1. North is indicated by arrows, and the scale bar corresponds to 1 km.

https://doi.org/10.5194/egusphere-2026-3669
Preprint. Discussion started: 23 September 2026

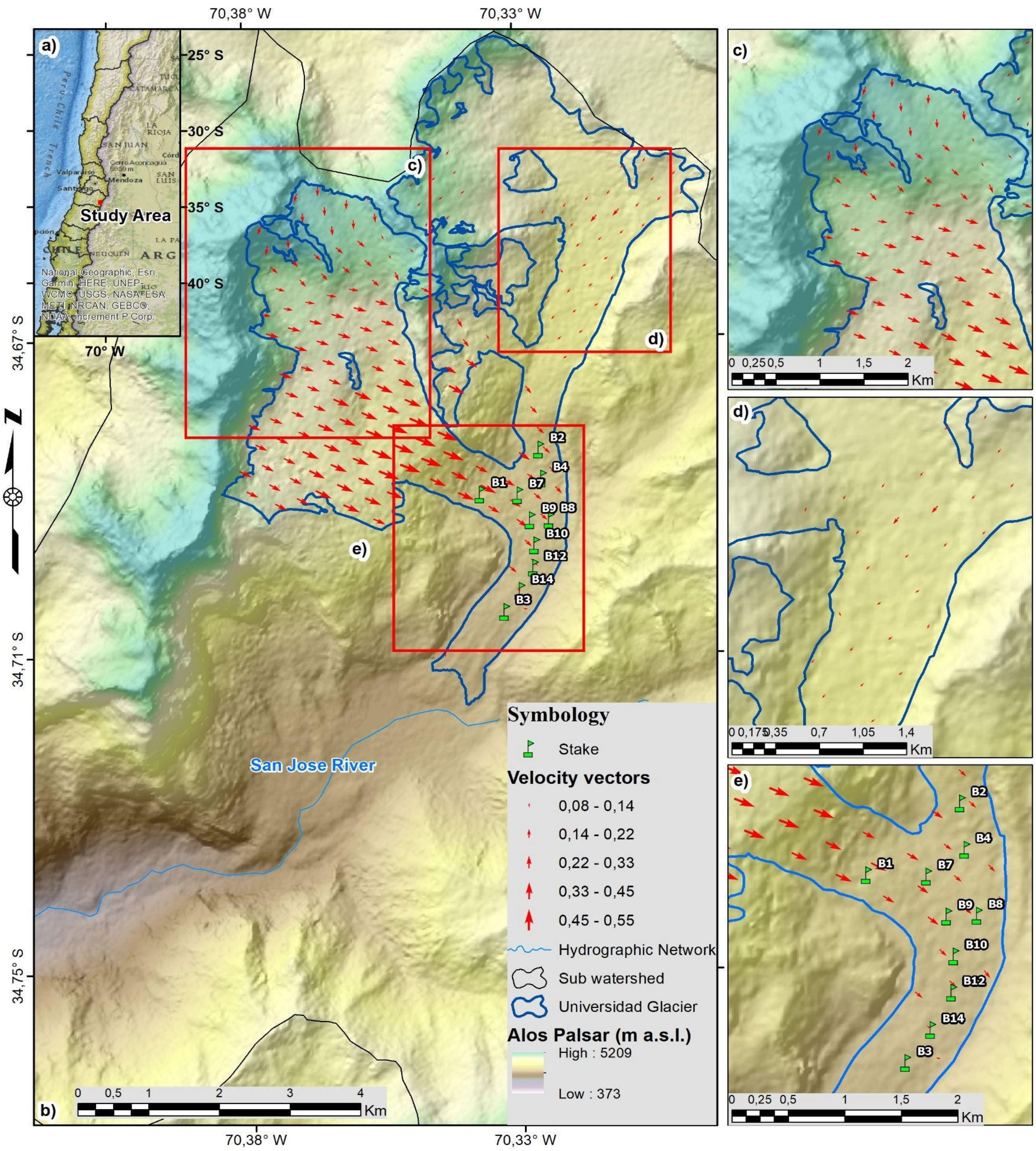

Figure 5. Surface velocity vector field of Universidad Glacier for the 06–18 March 2025 interval, derived from Sentinel-1 SAR offset tracking. (a) Regional context with glacier outline (blue) and ALOS PALSAR topography. (b) Full glacier extent. (c–e) Zoom panels showing stake positions (green) and velocity vectors (red, scaled by magnitude in m d^{-1}). Arrow length is proportional to velocity magnitude as indicated in the legend. Coordinate system: WGS84 geographic coordinates.

https://doi.org/10.5194/egusphere-2026-3669
Preprint. Discussion started: 23 September 2026

Figures 3 and 4 show the spatial distribution of surface velocities at Universidad Glacier derived from Sentinel-1 offset tracking for four 12-day pairs in each of the 2023–2024 and 2024–2025 ablation seasons. In both seasons, the highest velocities are concentrated in the icefall zone at the confluence of the tributary cirques, where values exceed 0.40 m d^{-1} in the April pairs, and decrease progressively upstream toward the accumulation zone (<0.10 m d^{-1}) and downstream along the lower tongue. The flow vectors delineate a well-defined central flowline that follows the glacier's main axis, confirming that ice motion is strongly constrained by glacier geometry and valley topography (Fig. 5).

The spatial pattern is consistent between seasons, but the magnitude of flow differs. In 2023–2024 (Fig. 3), the icefall and tongue display a broader zone of elevated velocities in December, and the 06–18 December 2023 pair also shows high values over the north-eastern accumulation cirque that are not repeated in any later pair and are most likely related to early-season snow conditions. In 2024–2025 (Fig. 4) the area of elevated flow speeds in the icefall is more localized and only becomes prominent in the March and April pairs. The upper glacier otherwise remains below the detection threshold in both seasons.

For visualization, the vector field was clipped to the mapped glacier outline and corrected for unrealistic flow directions following the procedure described in Sect. 3.1 (Fig. S4), reducing the 06–18 March 2025 field from 621 vectors in the full processing domain to 181 on-glacier vectors that clearly delineate the central flowline and its alignment with glacier geometry.

4.2 Velocity structure along the glacier flowline.

The along-centerline velocity profiles derived from Sentinel-1 offset tracking reveal a pronounced spatial structure in ice flow that is consistent across both ablation seasons, while differing substantially in magnitude from the long-term ITS_LIVE record (Fig. 6). In both 2023–2024 and 2024–2025, velocities increase progressively from the upper glacier (~0.05–0.10 m d^{-1} at 0–1.5 km) toward a well-defined maximum in the icefall zone at approximately 3.5–4.5 km from the head, before declining toward the glacier terminus (~0.03–0.06 m d^{-1} beyond 6.5 km in the season means). This spatial pattern a mid-glacier velocity maximum flanked by slower flow at both the upper accumulation area and the debris-covered lower terminus, is consistent with the expected dynamic structure of a valley glacier constrained by a pronounced bedrock step in the 3,500–3,000 m a.s.l. elevation band.

Season-mean velocities at the velocity maximum are markedly lower than the ITS_LIVE 1986–2025 long-term median. The Sentinel-1 season-mean profile for 2023–2024 peaks at 0.16 m d^{-1} (3.4 km from the head) and for 2024–2025 at 0.08–0.09 m d^{-1} (3.3 km; the lower value including, the higher excluding, the 36-day pair), compared to the ITS_LIVE long-term median of ~0.65 m d^{-1} and the 2020–2025 ITS_LIVE median of ~0.33 m d^{-1} at the same along-centerline position, i.e., 4–8 and 2–4 times lower, respectively. The comparison with Millan et al. (2022), who report a peak velocity of ~0.87 m d^{-1} for the 2017/18 season, further underscores the magnitude of the deceleration observed in recent years. This progressive reduction in peak velocities is also evident in the ITS_LIVE annual series (Fig. 6), where the highest velocities (~0.85–1.0 m d^{-1}) are associated with observations from the 1990s and early 2000s (warm-colored curves), while more recent years consistently show lower values, converging toward the 2020–2025 median. Notably, the ITS_LIVE annual profiles for

https://doi.org/10.5194/egusphere-2026-3669
Preprint. Discussion started: 23 September 2026

2023–2025 and the 2020–2025 median remain ~2–4 times higher than the Sentinel-1 season means for the same years (Fig. 6); the origin of this difference is examined in Sect. 5.4.

The interannual difference between the two Sentinel-1 seasons is modest in terms of peak magnitude but notable in the upper glacier: the 2023–2024 profile shows slightly higher velocities across the full centerline compared to 2024–2025, with the 2024–2025 profile at or below the detection threshold (0.05–0.08 m d^{-1}) in the upper section (0–1.5 km) and the 2023–2024 profile at ~0.15 m d^{-1} there, a value due entirely to the two December 2023 pairs (Sect. 4.1) and reduced to ≤0.10 m d^{-1} when they are excluded. Both profiles display large uncertainty bars at the velocity maximum (4–5 km), likely reflecting the high surface heterogeneity and crevassing in this sector, where offset-tracking coherence is reduced. The spatial confinement of detectable motion to the ablation tongue, and the near-stagnation of the upper glacier once the December 2023 pairs are set aside, contrasts with the ~0.13–0.16 m d^{-1} resolved there by ITS_LIVE (Fig. 6); the significance of this contrast, given the noise level of our product in the upper glacier, is discussed in Sect. 5.4.

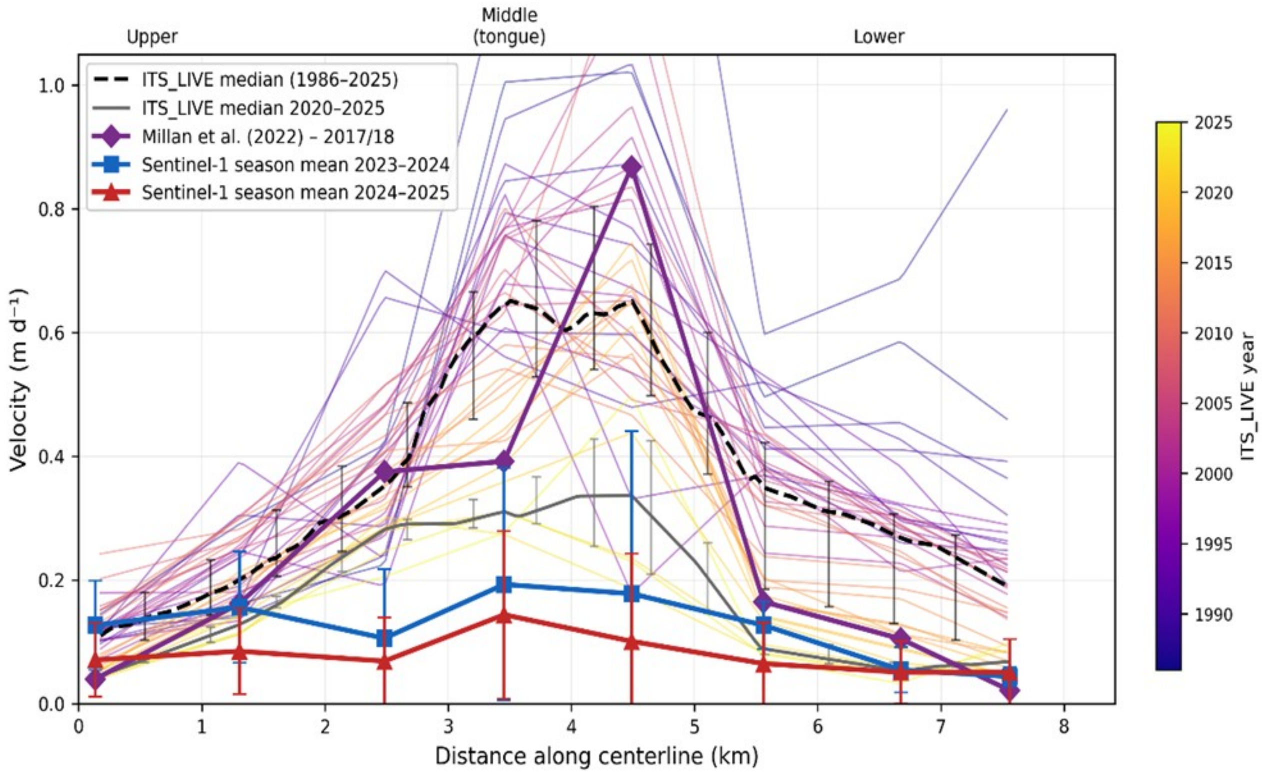

Figure 6. Along-centerline velocity profiles for Universidad Glacier, divided into upper, middle (tongue/icefall) and lower sectors. Thin colored lines show individual annual ITS_LIVE profiles (1986–2025; Gardner et al., 2025, Version 2), coloured by year, with medians for the full period (black dashed) and for 2020–2025 (gray). Millan et al. (2022) multi-annual velocities for 2017/18 (purple) and Sentinel-1 season means for 2023–2024 (blue) and 2024–2025 (red) are shown for comparison, with error bars indicating spatial/temporal variability. The velocity peak in the middle sector (~3.5–4.5 km) corresponds to the icefall zone (3,000–3,500 m a.s.l.). Sentinel-1 season means are computed from the LOWESS-smoothed centerline profiles deposited with this paper (Sect. 3.2).

https://doi.org/10.5194/egusphere-2026-3669
Preprint. Discussion started: 23 September 2026

4.3 GNSS velocity validation

To assess the accuracy of the Sentinel-1 SAR offset-tracking results, we compared the annual mean velocity at each stake (06 April 2024–28 April 2025 displacement; Sect. 3.3) with the Sentinel-1 season mean for 2024–2025 (December–April only) at the corresponding location (Fig. 7). Because the GNSS interval spans the full year, including the low-activity winter months, while the SAR value covers only the ablation season, the two are not coeval; this comparison therefore tests whether the SAR product reproduces the annual-scale spatial pattern and approximate magnitude of ice motion at the stakes, not whether it captures intra-seasonal variability, which the stake network cannot address at this survey frequency. The linear regression between the two yields $R^2 = 0.899$ ($n = 11$), a root-mean-square error of 0.022 m d^{-1} and a mean bias of −0.011 m d^{-1}, with SAR-derived values slightly underestimating the annual GNSS values. The regression slope, however, is 0.51: the SAR product reproduces the ranking of the stakes but underestimates the fastest stake (B1: GNSS 0.154 m d^{-1} vs. SAR 0.098 m d^{-1}, −36 %) by a much larger margin than the slower ones. Because B1 is the only stake moving faster than 0.08 m d^{-1}, it exerts strong leverage on the statistics: excluding it, the remaining ten stakes (0.01–0.07 m d^{-1}) yield $R^2 \approx 0.62$, a slope of ≈0.40 and RMSE = 0.015 m d^{-1}.

This level of agreement is comparable to reported accuracies of offset tracking applied to Sentinel-1 data over mountain glaciers (Nagler et al., 2015; Strozzi et al., 2002) for the velocity range sampled by the stakes. Three limitations must be stated explicitly. First, the validation sample is limited to $n = 11$ stakes, with an approximate 95% confidence interval for R^2 of [0.69, 0.97] that does not account for the leverage of B1. Second, the stakes are geographically concentrated in the lower glacier (latitudes ~−34.68° to −34.70°), below the icefall, and sample velocities of 0.01–0.16 m d^{-1} only; the icefall zone, where velocities of 0.2–0.5 m d^{-1} and the intra-seasonal changes discussed in Sect. 4.1 and 5 occur, is not covered by the stake network, so the RMSE of 0.022 m d^{-1} cannot be extrapolated to those areas. Third, the regression slope of 0.51 and the systematic negative bias across nearly all stakes (Fig. 7) indicate that the SAR product attenuates velocity gradients: the 200 m grid spacing, the 5 × 5 moving-window averaging and, above all, the 128 × 128 pixel (~1.3 km) registration window average the displacement field over an area much larger than the point-scale GNSS measurement, an effect expected to be largest precisely where local velocity gradients are steepest, i.e., at the icefall/tongue transition where stake B1 is located. The GNSS comparison therefore supports the spatial pattern and the order of magnitude of the SAR velocities in the lower glacier, but it also implies that the absolute magnitude of velocity maxima, and of their temporal changes, is likely underestimated by the present configuration (Sect. 4.2 and 5).

https://doi.org/10.5194/egusphere-2026-3669
Preprint. Discussion started: 23 September 2026

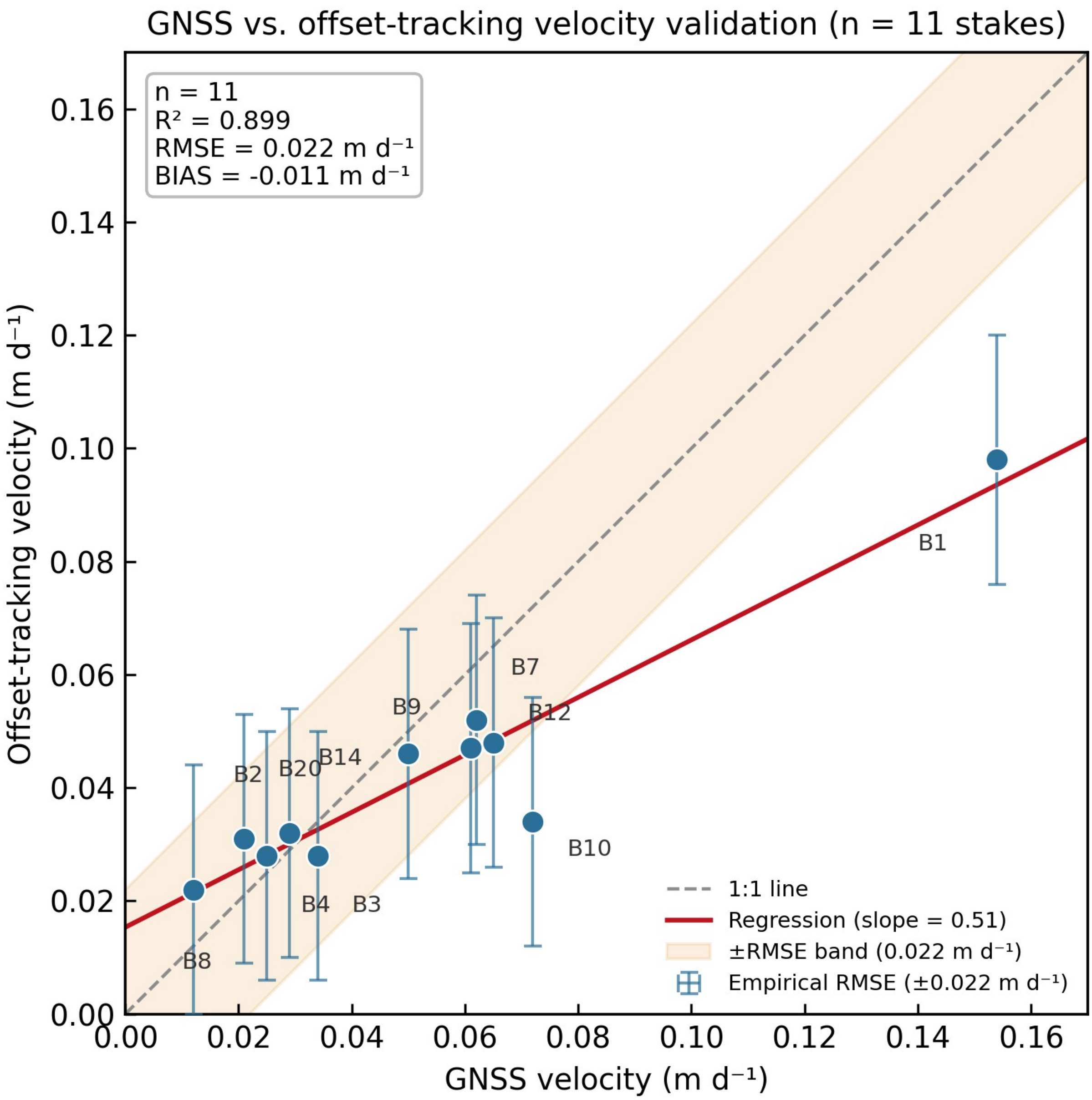

Figure 7. Validation of Sentinel-1 offset-tracking velocities against GNSS measurements at 11 ablation stakes during the 2024–2025 season: GNSS versus offset-tracking scatter plot with the 1:1 line (dashed), linear regression (red; slope = 0.51) and the empirical RMSE band (shaded; ±0.022 m d⁻¹). Overall statistics: R^2 = 0.899, RMSE = 0.022 m d⁻¹, bias = −0.011 m d⁻¹. The systematic negative bias and the largest discrepancy, at stake B1 in the fastest-moving location, are discussed in Sect. 4.3. As noted there, the RMSE band is derived from the same 11 points shown and is therefore an empirical, not an independent, uncertainty estimate; per-stake error bars reflecting the GNSS survey precision and the spatial variability of the Sentinel-1 season mean around each stake are identified as a priority revision pending confirmation of the source GNSS–SAR comparison (Sect. 4.3).

https://doi.org/10.5194/egusphere-2026-3669
Preprint. Discussion started: 23 September 2026

4.4 Analysis of velocities outside the glacier

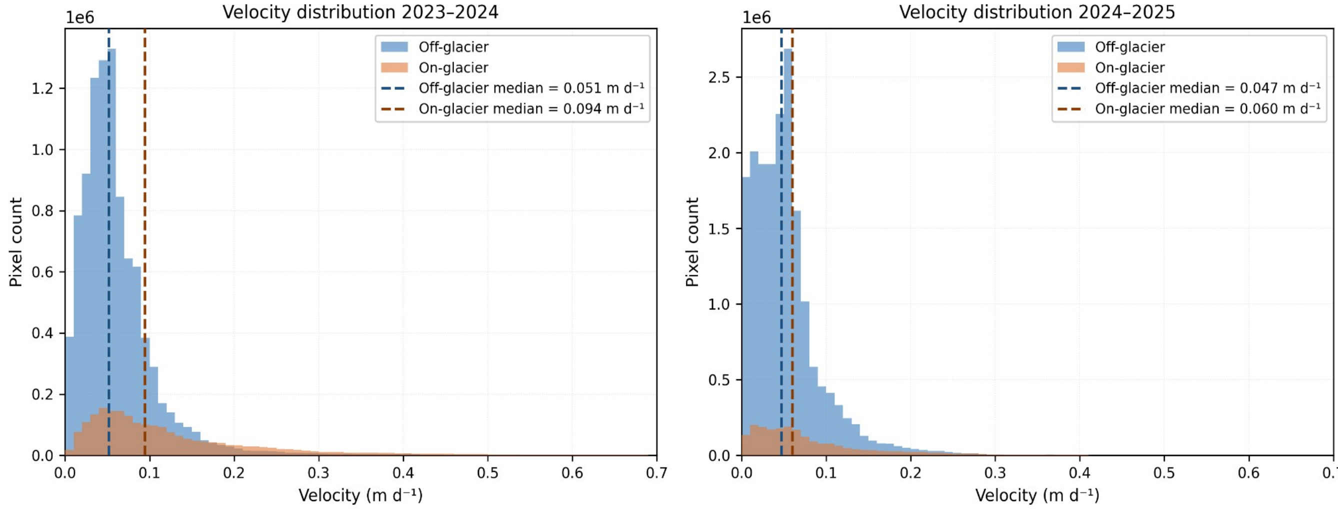

Figure 8. Velocity distribution of off-glacier (blue) and on-glacier (orange) pixels for the 2023–2024 (left) and 2024–2025 (right) seasons. Dashed lines indicate the median velocity for each distribution. The 90th percentile of the off-glacier distribution (~0.10 m d^{-1}) defines the detection threshold used in this study.

To further evaluate the reliability of the Sentinel-1 offset-tracking results, we analysed velocity distributions outside the glacier boundaries (Fig. 8), where no true surface displacement is expected. The off-glacier domain is the full reprojected raster extent per pair (~15 km × 15 km, excluding the on-glacier mask); this statistic is sensitive to the choice of domain, a narrower 1.5 km buffer around the margin yields P90 values ~1.3–2× higher, likely reflecting steeper, shadowed or seasonally snow-covered terrain closer to the ice, so the values below are a conservative, domain-averaged estimate. The off-glacier histograms are strongly right-skewed, with median velocities of 0.051 m d^{-1} (2023–2024) and 0.047 m d^{-1} (2024–2025), 90th percentiles of 0.095 and 0.082 m d^{-1}, and 95th percentiles of 0.115 and 0.098 m d^{-1}, consistent with the theoretical uncertainty of the configuration (~0.05–0.08 m d^{-1}) and defining the ~0.10 m d^{-1} detection threshold used throughout this study (applied to the on-glacier distributions in Sect. 4.1). The per-pair off-glacier 90th percentile is listed in Table 2 and Table S1, the latter the appropriate tool for identifying individual pairs affected by decorrelation (e.g., the April pairs, Sect. 4.1). Pixel counts (order 10^6) in Fig. 8 reflect the ~10 m export resolution of the source geocoded product rather than the ~200 m independent measurement spacing (~620 independent cells over the glacier; Sect. 3.1).

4.5 Comparison of Offset tracking with global velocity models.

To evaluate whether the short-term velocity variations observed at Universidad Glacier reflect broader flow conditions, we compared our Sentinel-1 offset-tracking (OT) results with velocities from the ITS_LIVE global product (Gardner et al., 2025a), as annual along-centerline profiles and multi-annual medians (Fig. 6). The ITS_LIVE data represent multi-annual

https://doi.org/10.5194/egusphere-2026-3669
Preprint. Discussion started: 23 September 2026

median flow conditions, whereas the OT velocity fields resolve intra-seasonal dynamics during the 2023–2024 and 2024–2025 ablation seasons.

Along the centerline, the ITS_LIVE 2020–2025 median (~0.33 m d⁻¹ at the icefall) lies between the Sentinel-1 season means (0.08–0.16 m d⁻¹) and the values of individual Sentinel-1 pairs during the fastest intervals (0.31–0.56 m d⁻¹ in the April pairs). A multi-annual median by construction averages out intra-seasonal variability; the Sentinel-1 series shows that, within one ablation season, velocities at the icefall vary by a factor of 2–3 between the February and March pairs, and by an order of magnitude if the April pairs are confirmed, a range that no annual or multi-annual product can represent, irrespective of whether the April values are eventually confirmed.

Comparing the two products by zone along the centerline (Fig. 6), the upper glacier shows the closest absolute agreement (both ≤0.15 m d⁻¹, within the Sentinel-1 noise level), whereas in the icefall and tongue the Sentinel-1 season means lie 0.17–0.25 m d⁻¹ below the ITS_LIVE 2020–2025 median and 0.49–0.57 m d⁻¹ below the 1986–2025 median. Only the 04–16 April 2024 pair exceeds the 2020–2025 median at the icefall (by up to +0.2 m d⁻¹); the 11–23 April 2025 pair (0.31 m d⁻¹) reaches but does not exceed it, and all other pairs lie 0.2–0.3 m d⁻¹ below it. The April excess exceeds both the empirical detection threshold (~0.10 m d⁻¹) and the theoretical uncertainty bound (0.05–0.08 m d⁻¹) but depends on pairs whose quality remains to be confirmed (Sect. 4.1). Whether these late-season values reflect enhanced basal sliding under increased water availability, as commonly observed in temperate glaciers, or decorrelation, is addressed in Sect. 5.2 and 5.3.

In addition to the comparison with ITS_LIVE, we evaluated our Sentinel-1 offset-tracking results against the regional glacier velocity product of Millan et al. (2022), which provides annual-scale velocities derived from feature tracking applied to Landsat and ASTER imagery (Fig. S6). The spatial distribution of flow speeds in the Millan et al. dataset shows a consistent pattern with our results, with the highest velocities concentrated in the icefall zone and flow acceleration occurring along the central flowline. Along the centerline, the Millan et al. product reaches ~0.85 m d⁻¹ (~310 m yr⁻¹) at the icefall for 2017–2018 (Fig. 6), i.e., roughly twice the maximum of any individual Sentinel-1 pair and 4–6 times the Sentinel-1 season means at the same location. The upper and mid-glacier sectors likewise exhibit low and moderate velocities, respectively, in both datasets. The flow vectors in the Millan et al. product align strongly with the directionality we observe in our multi-temporal velocity maps, confirming the stable, topographically constrained nature of the glacier's flow regime. Notably, however, Millan et al. represent an annual-scale (2017–2018) velocity state and therefore do not resolve the short-lived seasonal accelerations captured in our offset-tracking time series, further emphasizing the need for high-temporal-resolution SAR monitoring to detect melt-driven dynamic variability in valley glaciers of the Central Andes.

4.6 Air temperature during the two ablation seasons and relation to velocity

Over the 792 days for which the two temperature sources overlap, station and ERA5-Land daily mean temperatures are highly correlated (r = 0.93), with the station systematically warmer by +6.8 °C on average (Fig. S5), consistent with its markedly lower elevation than the glacierized catchment (Supplement Sect. S2); this offset does not affect the timing analysis below, which depends on relative, not absolute, temperature. Within the Sentinel-1 pair windows, both sources

https://doi.org/10.5194/egusphere-2026-3669
Preprint. Discussion started: 23 September 2026

place the seasonal temperature maximum of 2024–2025 in the 29 January–10 February 2025 window (station absolute maximum 27.9 °C on 8 February; ERA5-Land 15.5 °C on 9 February), and both show the coldest conditions of each season in the April pairs (station $\bar{T}$ = 7.2 °C in April 2025; ERA5-Land $\bar{T}$ = 1.3–1.5 °C in April 2024 and 2025). Cumulative positive degree-days (ERA5-Land basis, for consistency across both seasons) were nearly identical between the two seasons: 935.4 °C·day in 2023–2024 vs. 925.8 °C·day in 2024–2025.

Figure 9 compares the icefall/tongue mean velocity of each pair (centerline points beyond 3 km, LOWESS-smoothed as in Sect. 4.2) with the corresponding 7-day mean air temperature. In 2024–2025 the velocities of the December–early February pairs are flat within noise (0.031–0.034 m d^{-1}; Sect. 4.1), so that the seasonal temperature maximum (29 January–10 February) falls within this low, stationary interval; velocity then increases during the 06–18 March pair (0.062 m d^{-1}; +0.03 m d^{-1}, about 4–5 weeks after the thermal maximum, when the station 7-day mean had fallen to 12.0 °C) and, more markedly, during the 11–23 April pair (0.210 m d^{-1}; ~9–10 weeks after, at 7.2 °C). In 2023–2024, the first pair (06–18 December, 0.120 m d^{-1}) is the seasonal maximum, with the caveat on its quality noted in Sect. 4.1; velocity declines to a minimum in early February (04–16 February, 0.032 m d^{-1}) while station temperatures remain warm ($\bar{T}$ = 10.7–14.2 °C, January–March), and increases again in the 11–23 March pair (0.098 m d^{-1}). In neither season is velocity in phase with air temperature. The comparison in Fig. 9 uses the same digitized centerline and LOWESS smoothing as Fig. 2; station data are unavailable for the two December 2023 pairs and the April 2024 pair, for which the ERA5-Land estimate is used.

https://doi.org/10.5194/egusphere-2026-3669
Preprint. Discussion started: 23 September 2026

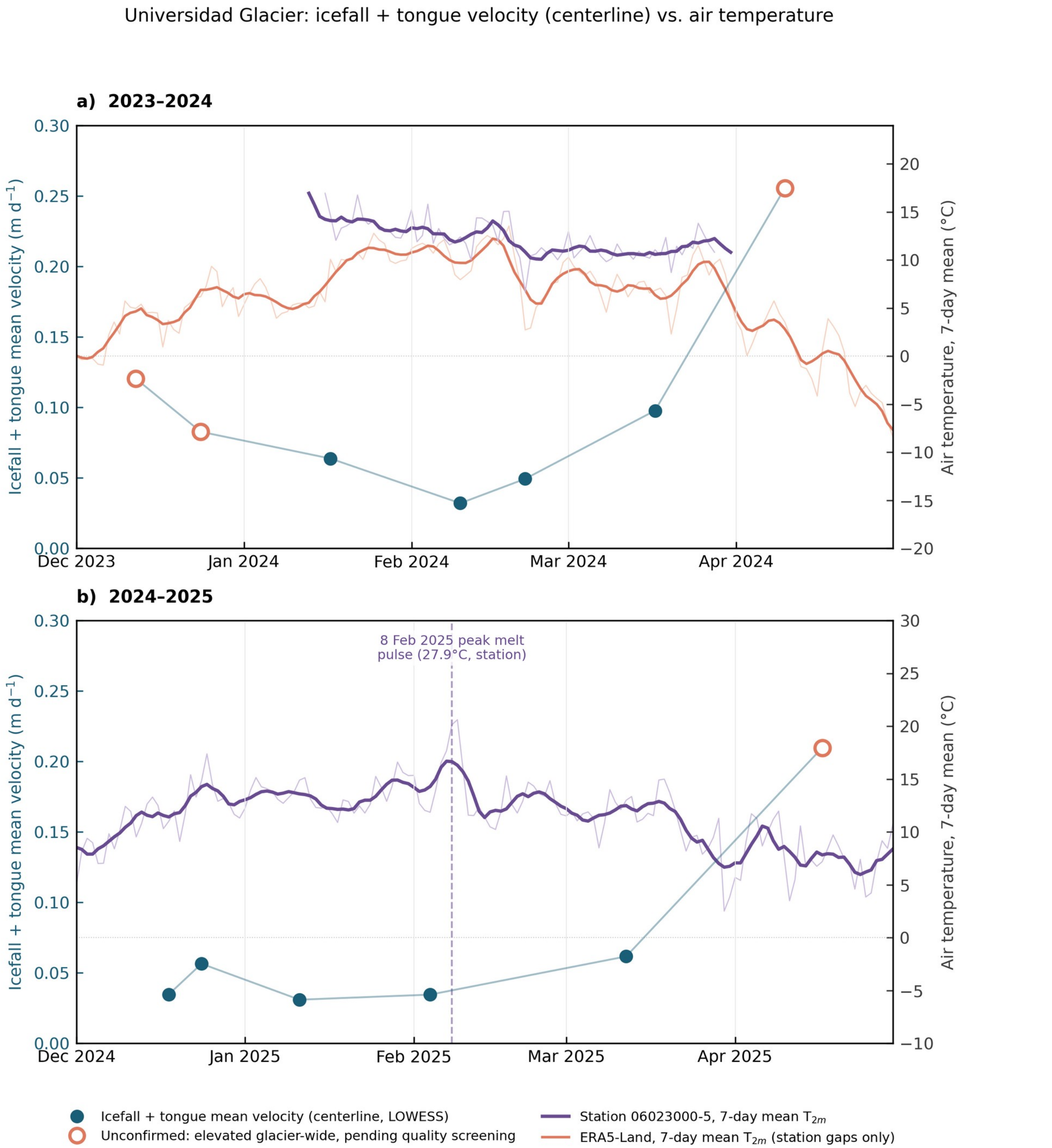

Figure 9. Mean surface velocity of the icefall and tongue (centerline points beyond 3 km) versus air temperature, for (a) 2023–2024 and (b) 2024–2025. Temperature is from DGA station 06023000-5 where available, and from ERA5-Land only for the intervals during which the station was offline (Dec 2023 and Apr 2024). Velocities are derived from the unfiltered Sentinel-1 offset-tracking rasters, sampled along the digitized centerline and LOWESS-smoothed (Sect. 4.2); the 36-day 10 February–18 March 2025 pair is not shown. Open circles mark the pairs treated as unconfirmed pending pair-specific quality assessment (06–18 and 18–30

https://doi.org/10.5194/egusphere-2026-3669
Preprint. Discussion started: 23 September 2026

December 2023, 04–16 April 2024 and 11–23 April 2025; Sect. 4.1). The vertical dashed line in (b) marks the station's seasonal absolute temperature maximum (8 Feb 2025, 27.9 °C).

5 Discussion

The results presented here constitute the first high-temporal-resolution characterization of surface velocity dynamics at Universidad Glacier. Four main findings emerge. First, the glacier exhibits a stable, geometry-controlled spatial flow structure, with a velocity maximum at the icefall, that is well represented by existing global velocity products (Sect. 5.1). Second, this structure is modulated by intra-seasonal velocity changes that are, by construction, invisible to multi-annual climatologies, but whose late-season component cannot yet be separated from decorrelation (Sect. 5.2). Third, in both seasons the icefall velocity is at the stable-terrain noise level in January–February and rises in March, 4–5 weeks after the seasonal temperature maximum in 2024–2025, i.e., not in phase with air temperature (Sect. 5.3). Fourth, season-mean velocities are 4–8 times lower than the long-term (1986–2025) ITS_LIVE median, although a factor of 2–4 of this difference is attributable to the spatial smoothing of our offset-tracking configuration (Sect. 5.4). Each of these findings is discussed below, followed by the implications for glacier hydrology and the outlook (Sect. 5.5).

5.1 Spatial flow structure and comparison with multi-annual velocity products

The spatial flow structure, with highest velocities at the icefall (~0.30–0.50 m d^{-1} in individual 12-day fields) decreasing toward the accumulation zone (<0.10 m d^{-1}) and along the lower tongue, is consistent across both ablation seasons and aligns with the ITS_LIVE climatology and the 2017–2018 product of Millan et al. (2022). The location of the velocity maximum and the flow vectors in all datasets reveal a coherent, topographically constrained central flowline. Such agreement indicates that the fundamental stress balance and ice-flux pathways of Universidad Glacier have remained stable over recent decades, even as the magnitude of flow has decreased.
The direct comparison between the Sentinel-1 offset-tracking velocities and the multi-annual velocity field of Millan et al. (2022) (Fig. S6) further supports this interpretation. Given that both datasets are strongly non-normally distributed (D'Agostino test, $p < 10^{-150}$), Spearman's rank correlation (ρ) and Kendall's τ are reported as the primary association metrics, which are robust to non-normality and do not assume a linear relationship. For the March 2024 window (11–23 March), the regression of Millan et al. velocities on offset-tracking velocities yields a slope of 0.55 with $\rho = 0.079$ and $\tau = 0.060$, whereas for March 2025 (06–18 March) the slope is 0.77 with $\rho = 0.127$ and $\tau = 0.086$ (Fig. S6). These effect sizes indicate a weak monotonic association; the statistical significance ($p < 10^{-76}$) is a consequence of the very large sample size ($n \approx 55{,}000$ pixels, obtained by resampling the 200 m offset-tracking grid to the Millan et al. grid, so that the number of independent samples is closer to ~600) and should not be interpreted as evidence of a strong relationship. The low correlation coefficients are expected and physically meaningful: the Millan et al. (2022) dataset represents an annual (2017–2018) velocity state, while the offset-tracking captures intra-seasonal variability at bi-weekly timescales, so point-to-point agreement is not anticipated. In both seasons, the Millan et al. (2022) velocities exceed the offset-tracking velocities over

https://doi.org/10.5194/egusphere-2026-3669
Preprint. Discussion started: 23 September 2026

most of the glacier (points above the 1:1 line in Fig. S6), with the largest dispersion at low offset-tracking speeds where matching noise dominates. Despite the weak pixel-scale correlations, both datasets are spatially consistent in identifying the icefall zone as the highest-velocity sector, with the systematic offset reflecting both the lower velocities of 2024–2025 relative to 2017–2018 and the smoothing of the offset-tracking configuration, and the residual scatter reflecting sub-seasonal velocity fluctuations and matching noise.

Part of the observed dispersion between the offset-tracking velocities and the Millan et al. (2022) multi-annual product can also be explained by their temporal mismatch. The Millan dataset represents velocities for 2017–2018, while the offset-tracking measurements correspond to specific ablation-season intervals in 2024 and 2025, years with distinct melt conditions and hydrological forcing, potentially influenced by the intense ENSO event that affected the Central Andes in 2023. Because the multi-annual velocities intrinsically smooth interannual variability, including anomalous melt seasons or shifts in snow cover, they cannot reproduce event-scale accelerations captured by the SAR time series. This temporal offset adds to the scatter at low and intermediate velocities, so that the discrepancies combine real short-term and interannual variability with the methodological differences discussed above.

The comparison between Sentinel-1 offset tracking and ITS_LIVE leads to the same conclusion. While ITS_LIVE accurately captures the structural velocity regime, its near-constant values contrast with the pronounced intra-seasonal variability resolved by the Sentinel-1 time series. This discrepancy is strongest at the icefall, where the April 2024 pair exceeds the ITS_LIVE 2020–2025 median by up to +0.2 m d^{-1} while the January–February pairs of both seasons fall 0.25–0.30 m d^{-1} below it. Because the Millan et al. dataset also reflects annual-scale (2017–2018) flow conditions, it likewise does not express these short-lived accelerations. Together, these comparisons indicate that long-term velocity products effectively characterize glacier geometry–controlled flow, but do not capture meltwater-driven, transient dynamic responses.

Taken together, this comparison yields a central result of this study: ITS_LIVE provides a reliable representation of the glacier's long-term, geometry-controlled flow structure, but it cannot, by construction, resolve intra-seasonal velocity changes such as those recorded here at the icefall (a factor of 2–3 between February and March, and up to an order of magnitude if the April pairs are confirmed). This is not a deficiency of ITS_LIVE per se, but a reflection of the temporal averaging inherent in any multi-annual product. The implication for glacier hydrology is that the melt-related velocity changes most likely to influence subglacial water routing occur on timescales that only repeat-pass SAR time series can capture, provided that individual pairs are screened for decorrelation and that the spatial resolution of the matching configuration is adequate for the width of the fast-flowing zone. High-temporal-resolution SAR monitoring is therefore complementary to, and necessary alongside, global products for understanding the dynamic behavior of melt-sensitive Andean glaciers.

5.2 Intra-seasonal velocity changes: dynamic signal or decorrelation?

Superimposed on this stable flow architecture, however, are short-term velocity fluctuations at sub-seasonal scales. Contrary to our initial reading of the velocity fields, the two ablation seasons do not show contrasting timing: in both, the icefall and

https://doi.org/10.5194/egusphere-2026-3669
Preprint. Discussion started: 23 September 2026

tongue velocity is at the stable-terrain noise level in January–February and increases in March and April (Fig. 9). The two seasons differ in the December level (0.12 vs. 0.03–0.06 m d^{-1}), which in 2023–2024 rests on pairs whose quality is uncertain (Sect. 4.1), and in the amplitude of the late-season increase. A sensitivity of the glacier to variations in meltwater supply and to the efficiency of subglacial drainage, mechanisms widely recognized as controls on sliding velocity in temperate and polythermal glaciers, is one candidate explanation for this pattern; a seasonal change in surface conditions affecting SAR coherence is another, and the two must be separated before the pattern is interpreted dynamically.

The agreement between offset-tracking velocities and GNSS stake measurements (R^2 = 0.899, RMSE = 0.022 m d^{-1}, slope = 0.51) confirms that the spatial pattern of velocities in the lower glacier is real and not an artifact of the satellite processing chain; it does not, however, validate the temporal changes at the icefall, which occur at velocities and in a sector not sampled by the stakes (Sect. 4.3). Establishing whether large valley glaciers in semiarid environments experience rapid, reversible changes in ice motion in response to seasonal meltwater input therefore requires, in addition to the present time series, stake or continuous GNSS observations in the icefall zone during the intervals of change.

Based on the two seasons analyzed, Universidad Glacier illustrates that large valley glaciers in semiarid mountain environments can exhibit intra-seasonal velocity changes of a factor of 2–3 at the icefall within a single ablation season. The only change that is unambiguously above the noise level in both seasons is the February-to-March increase at the icefall (from 0.03–0.05 to 0.09–0.14 m d^{-1} at the velocity maximum; icefall/noise ratios rising from ≈1 to 2.7–4.4, Table S1); the December-to-February decline of 2023–2024 (−0.09 m d^{-1} in the icefall/tongue mean) depends on December pairs of uncertain quality, and the larger April increases, if confirmed, would be of the same order as the seasonal velocity changes documented on temperate glaciers, but their attribution to meltwater forcing remains to be demonstrated with a longer time series and pair-level quality control.

5.3 Hydrometeorological context and a working hypothesis for the lagged response

The near-identical cumulative positive degree-days of the two seasons (Sect. 4.6) indicate statistically equivalent total thermal forcing. The difference in December velocity between the two seasons, and the different amplitude of their late-season increase, therefore cannot be explained by a difference in the amount of surface melt; if meltwater is involved, its timing and routing, rather than its total volume, must be responsible.

Taken at face value, the 2024–2025 sequence described in Sect. 4.6, velocity at the noise floor at peak melt, increase after air temperature has fallen, is the opposite of an instantaneous response to surface melt. One physically based explanation is a delayed subglacial hydrological response: meltwater generated during the early-February thermal pulse may have required several weeks to reach the bed and reorganize the subglacial drainage system, producing a transient increase in basal water pressure and enhanced sliding that outlasted the atmospheric forcing that initiated it, a pattern documented in temperate and polythermal glacier hydrology (e.g., Bartholomew et al., 2010; Sole et al., 2011; Schoof, 2010). An alternative, non-dynamic explanation is that the March and, particularly, the April pairs are affected by decorrelation associated with autumn snowfall and falling temperatures, which biases offset estimates toward higher, spatially incoherent values across the entire glacier, a pattern consistent with the glacier-wide increase seen in Figs. 2B and 4 for April 2025 and with the April 2024 pair, which shows the same signature. With only the +0.03 m d^{-1} increase of the March pair (in the icefall/tongue mean; +0.05 m d^{-1} at the icefall maximum) falling within the ablation season proper, and this increase lying below the detection threshold although 2–4 times above the stable-terrain noise (Table S1), the present data cannot discriminate between the two explanations. A more direct test is available from the station's snow-depth sensor (Sect. 3.5): it records essentially no change (±0.2 cm, within instrumental noise) during the 06–18 March and 11–23 April 2025 windows, giving no station-based evidence of fresh snowfall there; the 04–16 April 2024 window has no station data (offline) and cannot be checked. Taken at face value this argues against decorrelation for the 2025 pairs, but the station sits 5 km from the glacier at a markedly lower elevation (Sect. 4.6), so a light, dry snowfall confined to the glacier surface, sufficient to reduce SAR coherence without registering on a point sonic sensor downslope, cannot be excluded. The two explanations therefore remain undiscriminated for the flagged pairs as a set, though the snow record somewhat favours the subglacial-hydrology interpretation where it is available.

The 2023–2024 decline under sustained warmth (Sect. 4.6) is the expected signature of a transition from an inefficient, distributed drainage configuration to a more efficient, channelized one as the season progresses. However, because no pair precedes 6 December, the speed-up that would have preceded this decline is not observed, and we cannot exclude that the elevated December values themselves reflect early-season snow conditions, as suggested by the anomalously high velocities retrieved over the north-eastern accumulation cirque in the same pair (Fig. 3); with the two December pairs set aside, the decline is only established from the 11–23 January pair (0.064 m d^{-1}) to February (0.032 m d^{-1}), a difference within the detection threshold. The March 2024 increase mirrors that of March 2025, so the two seasons are best described as one sequence with different amplitudes rather than as contrasting behaviours.

We stress that this hydrometeorological comparison remains exploratory: it relies on unfiltered offset-tracking velocities averaged along the centerline beyond 3 km, on a single ablation-season cycle per year, and on pairs whose late-season values have not passed a pair-specific quality screening. The lag hypothesis is consistent with two independent and closely agreeing temperature records for the timing of the 2024–2025 melt pulse, but it rests on one event in one season and on a velocity change at the detection limit, and should be regarded as a physically plausible working hypothesis motivating the surface energy-balance monitoring now underway at the site (Sect. 3.5; Data Availability), rather than as a confirmed causal result. ERA5-Land's ~9–11 km grid spacing also does not resolve the glacier's internal elevation gradient (2500–4540 m a.s.l.); no lapse-rate correction was applied, so the temperature series should be read as representative of catchment-average synoptic forcing rather than a spatially distributed melt model.

5.4 Multidecadal deceleration: methodological and glaciological components

Season-mean velocities at the icefall (0.16 and 0.08–0.09 m d^{-1}) are 4–8 times lower than the ITS_LIVE 1986–2025 median and 6–12 times lower than the peak velocities of the 1990s (Sect. 4.2). Before interpreting this difference as glaciological change, its methodological component must be isolated. The ITS_LIVE annual profiles for 2023–2025 and the 2020–2025 median remain ~2–4 times higher than the Sentinel-1 season means for the same years, even though ablation-season velocities are expected to equal or exceed annual means. This indicates that part of the difference between our product and ITS_LIVE is methodological, most plausibly the spatial smoothing introduced by the 128-pixel (~1.3 km) matching window, the 200 m grid and the 5×5 moving-window average over a velocity maximum only a few hundred metres wide consistent with the regression slope of 0.51 against GNSS (Sect. 4.3). Likewise, the upper glacier moves more slowly in our product (0.07–0.13 m d^{-1}) than in ITS_LIVE (~0.13–0.16 m d^{-1}), which could reflect reduced driving stress associated with ongoing mass loss and thinning; but because these values lie within the noise level of our product, the contrast cannot be quantified and should not be read as evidence of dynamically decoupled flow regimes. Two method-independent checks could resolve this without relying on the smoothing correction proposed here: (i) applying the present offset-tracking pipeline to Sentinel-1 pairs from 2015–2018, overlapping directly with the Millan et al. (2022) epoch, and (ii) comparing against individual ITS_LIVE image-pair velocities (rather than the annual mosaics used above) for 2023–2025, which share a temporal sampling closer to our 12-day pairs. Both are identified as priorities for follow-up work; in their absence, the 4–8-fold difference reported here is best read as a difference between velocity products with a probable, but not yet isolated, glaciological component, rather than as a quantified deceleration.

Allowing for a methodological factor of 2–4, the Sentinel-1 profiles still indicate that Universidad Glacier is operating well below the dynamic intensity recorded since the late 1980s. This residual deceleration is consistent with the sustained negative mass balance and glacier thinning reported for the Central Andes over recent decades (Hugonnet et al., 2021; Podgórski et al., 2023), and suggests that ice flux toward the ablation area is diminished relative to the late twentieth century. We propose that this multidecadal trend and the intra-seasonal fluctuations documented above are not independent findings but two timescale-dependent expressions of the same underlying control: the glacier's dynamic response to meltwater availability, mediated by the state of its subglacial drainage system. A thinner, less active glacier with reduced meltwater production (consistent with the sustained negative mass balance reported by Podgórski et al., 2023) would be expected to generate smaller and less frequent basal-pressure pulses of the kind described above, plausibly allowing efficient, channelized drainage to persist for longer periods and dampening the high-velocity, distributed-drainage events that dominated the glacier's dynamics in the 1990s (when ITS_LIVE records velocities 6–12 times higher than our season means, of which a factor of 2–4 may be methodological). Under this interpretation, the present-day intra-seasonal fluctuations (+0.03 to +0.07 m d^{-1} in the icefall/tongue mean between February and March; up to +0.1 m d^{-1} at the velocity maximum) are best understood as a smaller-amplitude, present-day analogue of the same meltwater-drainage coupling that historically produced substantially larger seasonal and multi-annual velocity variations. We present this as a testable hypothesis for future work rather than a demonstrated result: confirming it will require longer SAR time series, distributed energy-balance modeling, and direct subglacial-hydrology observations (e.g., moulin or borehole monitoring) that are beyond the scope of the present two-season dataset.

5.5 Implications for glacier hydrology and outlook

https://doi.org/10.5194/egusphere-2026-3669
Preprint. Discussion started: 23 September 2026

These findings have broader implications for glacier–hydrology interactions in water-stressed mountain basins. Hydrologically driven velocity short-term accelerations may influence not only ice flow but also the timing and buffering of meltwater release, with potential effects on late-season runoff a critical water source for downstream communities within the Rapel River basin, which receives meltwater contributions from Universidad Glacier. Understanding such feedbacks is therefore essential for hydrological forecasting and water-resource management in regions where cryospheric inputs are increasingly vulnerable to climate change.

To evaluate these hydrological feedbacks directly, we also examined discharge from the nearest operational gauge, Río Tinguiririca bajo Los Briones (BNA 06028001-0, ~46 km downstream, contributing area on the order of 10^3 km^2; Supplement Figs. S1–S2). Daily discharge follows a smooth recession through both ablation seasons with no signature of the intra-seasonal velocity changes, and the 30-minute record shows a pronounced diurnal cycle (mean relative amplitude 33–42%) confirming a melt-dominated regime at the basin scale. We regard the absence of a glacier-specific signal as expected rather than inconclusive: the 24.91 km^2 glacier is a small fraction of the gauged area, so any glacier-derived pulse is diluted by the basin-integrated snowmelt signal (cf. Ayala et al., 2020). Records from the gauge closest to the glacier outlet (Río Tinguiririca after the Azufre confluence, BNA 06025001-4, ~26 km downstream) could not be obtained for this manuscript and remain a priority: a dedicated follow-up study will combine them with a velocity product screened pair by pair for decorrelation to evaluate whether melt-driven velocity changes at Universidad Glacier produce detectable hydrological signatures closer to the source, and on what timescale. This glacier–hydrology integration is a critical next step toward quantifying the dynamic contribution of Universidad Glacier to water availability in the Rapel basin.

6. Conclusions

Universidad Glacier currently appears to be flowing markedly more slowly than in the ITS_LIVE record: season-mean velocities during 2023–2024 and 2024–2025 (0.16 and 0.08–0.09 m d^{-1} at the icefall velocity maximum) are approximately 4–8 times lower than the ITS_LIVE 1986–2025 median and 6–12 times lower than the peak velocities recorded in the 1990s. Part of this difference (a factor of 2–4, as indicated by the comparison with ITS_LIVE for 2020–2025 and by the regression slope of 0.51 against GNSS) is attributable to the spatial smoothing of our offset-tracking configuration; whether the remainder reflects a genuine multidecadal slowdown, which would be consistent with the sustained negative mass balance and glacier thinning reported across the Central Andes, cannot be confirmed from the present two-season, single-configuration dataset. We therefore present this as a probable but as yet unquantified trend rather than an established result, pending the method-agnostic checks proposed in Sect. 5.4. The glacier retains a stable, geometry-controlled spatial flow structure, with the highest surface velocities at the icefall (3,000–3,500 m a.s.l.) and lower values both in the accumulation zone and along the debris-covered lower tongue. This structural pattern is consistent across both seasons studied and aligns with the flow fields of ITS_LIVE and Millan et al. (2022); whether the glacier's large-scale stress balance and ice-flux

https://doi.org/10.5194/egusphere-2026-3669
Preprint. Discussion started: 23 September 2026

pathways have remained stable despite a possible velocity decline, or have themselves adjusted, is a further question for the follow-up work identified above.

Superimposed on this stable configuration are intra-seasonal velocity changes at the icefall. In both seasons the icefall velocity is at the stable-terrain noise level in January–February and increases by a factor of 2–3 in March; the higher December 2023 values and the larger April increases of both seasons coincide with elevated velocities over the whole glacier and remain unconfirmed. Cumulative positive degree-days were nearly identical between the two seasons, so that the differences between them lie in the December level and in the amplitude of the late-season increase, rather than in the magnitude of thermal forcing.

The comparison with in situ and ERA5-Land air temperature (Sect. 4.6 and 5.3) confirms that velocity was not in phase with air temperature: in 2024–2025, velocity remained at the noise floor through the seasonal temperature maximum (8 February 2025) and increased only weeks later, after temperatures had fallen. This lag is consistent with, but does not yet confirm, a delayed subglacial-drainage response (Sect. 5.3); confirming it will require pair-level quality screening of the SAR time series, GNSS observations in the icefall zone, and the surface energy-balance monitoring now underway.

The comparison between Sentinel-1 offset-tracking velocities and in situ GNSS stake measurements ($R^2 = 0.899$, RMSE = 0.022 m d^{-1}, slope = 0.51, n = 11) confirms the spatial pattern of velocities in the lower glacier over the range 0.01–0.16 m d^{-1}, but also reveals a systematic underestimation of the fastest stake that must be taken into account when interpreting absolute velocities at the icefall; it supports the use of high-temporal-resolution SAR offset tracking for monitoring remote, high-elevation glaciers provided that the matching configuration is adapted to the width of the fast-flowing zone.

Comparisons with ITS_LIVE and the product of Millan et al. (2022) show that global and multi-annual velocity datasets effectively represent the structural flow regime but cannot, by construction, capture intra-seasonal velocity changes resolved by repeat-pass offset tracking. The difference in reference period (2017–2018 for Millan et al.) also contributes to the observed dispersion, further emphasizing the need for monitoring strategies capable of resolving transient glacier dynamics.

Most broadly, this work provides a two-season, high-temporal-resolution velocity baseline for Universidad Glacier and identifies the observational requirements, namely pair-by-pair quality screening, a matching configuration adapted to the width of the fast-flowing zone, and in situ observations at the icefall, needed to establish whether the intra-seasonal velocity changes documented here are melt-driven. If confirmed, these are precisely the signals most relevant for subglacial water routing and the timing of meltwater release into the Rapel River basin, a critical water source for downstream communities, and their quantification would be a prerequisite for improved hydrological forecasting under ongoing climate change in semiarid mountain regions. The velocity baseline established here provides the foundation for future multi-year analyses that will be necessary to distinguish genuine interannual trends from short-term variability. Integrating the growing SAR time series with the temperature, precipitation and discharge records now being assembled will be essential for understanding glacier–hydrology feedbacks in this water-sensitive mountain region.

7. Acknowledgments

We thank María del Pilar Adriasola and Roberto Frank for facilitating access to the study area. We are also grateful to Brandon Navarro, Ivo Fercovic, Héctor Vargas, and Antonio Díaz (Respiro Andino tourism agency) for their valuable assistance during fieldworks. This study is part of the outcomes of the project "Asesoría y consultoría de apoyo para el monitoreo de detalle del Glaciar Universidad, Región de O'Higgins, Macrozona Centro 2024-2025), funded by General Water Directorate (DGA) of the Chilean Ministry of Public Works (MOP).

8. Code and data availability

The Sentinel-1 GRD imagery used in this study is freely available from the Copernicus Data Space Ecosystem (https://dataspace.copernicus.eu). ITS_LIVE velocities were obtained from the ITS_LIVE application (https://its-live.jpl.nasa.gov; Gardner et al., 2025a): Version 2 annual mosaics for 1985–2022 (Gardner et al., 2025b, https://doi.org/10.5067/JQ6337239C96) and Level 2 image-pair velocities for 2023–2025, which for this period are derived from optical (Landsat 8/9 and Sentinel-2) pairs only. GNSS stake data will be made available upon reasonable request. ERA5-Land data were accessed via Google Earth Engine (ECMWF/ERA5_LAND/HOURLY). Hourly meteorological data from DGA station 06023000-5 ("Glaciar Universidad", satellite telemetry network, operating intermittently since November 2022) were obtained from the Dirección General de Aguas real-time monitoring platform (https://snia.mop.gob.cl). A separate automatic weather station (AWS) and surface energy-balance monitoring program, providing full radiation and turbulent-flux components for distributed melt modeling, was established at the site in October 2025 and is ongoing; these data will be incorporated in a follow-up analysis. The Sentinel-1 velocity fields (GeoTIFF, 10 m, EPSG:32719), the along-centerline profiles and the glacier outline and centerline presented here are deposited at Zenodo (https://doi.org/10.5281/zenodo.22774316). Daily-mean and 30-minute instantaneous discharge for the Río Tinguiririca bajo Los Briones gauge (BNA 06028001-0) were obtained from the same DGA platform and are analysed in Supplement Figs. S1–S2. Discharge records from the closer Río Tinguiririca after the Azufre confluence gauge (BNA 06025001-4) were requested but not obtained; these remain a priority for future work.

9. Author contributions

Conceptualization: CU, AG, HFN, JB, PP; Formal analysis and Methodology: CU, AG, JB, JR; Writing – original draft preparation: CU; Writing – review & editing: all authors.

https://doi.org/10.5194/egusphere-2026-3669
Preprint. Discussion started: 23 September 2026

10. Financial support

This work was supported by the project "Asesoría y consultoría de apoyo para el monitoreo de detalle del Glaciar Universidad, Región de O'Higgins, Macrozona Centro 2024-2025) carried out by the Instituto de Ciencias Agroalimentarias, Animales y Ambientales (ICA3) at the Universidad de O'Higgins (UOH) and funded by General Water Directorate (DGA) of the Chilean Ministry of Public Works (MOP).

11. Competing interests

The authors declare that they have no conflict of interest.

12. References

Ayala, Á., Farías-Barahona, D., Huss, M., Pellicciotti, F., McPhee, J., and Farinotti, D.: Glacier runoff variations since 1955 in the Maipo River basin (semi-arid Andes of Chile), The Cryosphere, 14, 2005–2027, https://doi.org/10.5194/tc-14-2005-2020, 2020.

Barcaza, G., Nussbaumer, S. U., Tapia, G., Valdés, J., García, J.-L., Videla, Y., Albornoz, A., and Arias, V.: Glacier inventory and recent glacier variations in the Andes of Chile, South America, Ann. Glaciol., 58, 166–180, https://doi.org/10.1017/aog.2017.28, 2017.

Bartholomew, I., Nienow, P., Mair, D., Hubbard, A., King, M. A., and Sole, A.: Seasonal evolution of subglacial drainage and acceleration in a Greenland outlet glacier, Nat. Geosci., 3, 408–411, https://doi.org/10.1038/ngeo863, 2010.

Cuffey, K. M. and Paterson, W. S. B.: The Physics of Glaciers, 4th edn., Elsevier, Amsterdam, ISBN 978-0-12-369461-4, 2010.

Dirección General de Aguas (DGA): Red de estaciones hidrometeorológicas, Estación 06023000-5 Glaciar Universidad en Río San Andrés, Ministerio de Obras Públicas, Chile, https://snia.mop.gob.cl, data accessed 2026.

DGA and UOH (Dirección General de Aguas and Universidad de O'Higgins): Monitoreo Glaciológico del Glaciar Universidad, Región del Libertador Bernardo O'Higgins, 2024–2025, Informe final, Universidad de O'Higgins (ICA3) and Dirección General de Aguas, Ministerio de Obras Públicas, Chile, https://repositoriodirplan.mop.gob.cl/biblioteca/handle/20.500.12140/220176, 2026.

Falaschi, D., Kääb, A., Paul, F., Tadono, T., Rivera, J. A., and Lenzano, L. E.: Brief communication: Collapse of 4 Mm^3 of ice from a cirque glacier in the Central Andes of Argentina, The Cryosphere, 13, 997–1004, https://doi.org/10.5194/tc-13-997-2019, 2019.

https://doi.org/10.5194/egusphere-2026-3669
Preprint. Discussion started: 23 September 2026

Farinotti, D., Huss, M., Fürst, J. J., Landmann, J., Machguth, H., Maussion, F., and Pandit, A.: A consensus estimate for the ice thickness distribution of all glaciers on Earth, Nat. Geosci., 12, 168–173, https://doi.org/10.1038/s41561-019-0300-3, 2019.

Fernández, H., García, J.-L., Nussbaumer, S. U., Geiger, A. J., Gärtner-Roer, I., Pérez, F., Tikhomirov, D., Christl, M., and Egli, M.: De-icing landsystem model for the Universidad Glacier (34° S) in the Central Andes of Chile during the past ~660 years, Geomorphology, 400, 108096, https://doi.org/10.1016/j.geomorph.2021.108096, 2022.

Fernández-Navarro, H., García, J.-L., Nussbaumer, S. U., Tikhomirov, D., Pérez, F., Gärtner-Roer, I., Christl, M., and Egli, M.: Fluctuations of the Universidad Glacier in the Andes of central Chile (34° S) during the latest Holocene derived from a ^{10}Be moraine chronology, Quaternary Sci. Rev., 300, 107884, https://doi.org/10.1016/j.quascirev.2022.107884, 2023.

Flores-Aqueveque, V., Rojas, M., Aguirre, C., Arias, P. A., and González, C.: South Pacific Subtropical High from the late Holocene to the end of the 21st century: Insights from climate proxies and general circulation models, Clim. Past, 16, 79–99, https://doi.org/10.5194/cp-16-79-2020, 2020.

Gardner, A. S., Greene, C. A., Kennedy, J. H., Fahnestock, M. A., Liukis, M., López, L. A., Lei, Y., Scambos, T. A., and Dehecq, A.: ITS_LIVE global glacier velocity data in near-real time, The Cryosphere, 19, 3517–3533, https://doi.org/10.5194/tc-19-3517-2025, 2025a.

Gardner, A. S., Fahnestock, M., Greene, C. A., Kennedy, J. H., Liukis, M., López, L. A., and Scambos, T.: MEaSUREs ITS_LIVE Regional Glacier and Ice Sheet Surface Velocities, Version 2, NASA National Snow and Ice Data Center Distributed Active Archive Center, https://doi.org/10.5067/JQ6337239C96, 2025b.

Garreaud, R. D.: The Andes climate and weather, Adv. Geosci., 22, 3–11, https://doi.org/10.5194/adgeo-22-3-2009, 2009.

Garreaud, R. D., Boisier, J. P., Rondanelli, R., Montecinos, A., Sepúlveda, H. H., and Veloso-Águila, D.: The Central Chile Mega Drought (2010–2018): A climate dynamics perspective, Int. J. Climatol., 40, 421–439, https://doi.org/10.1002/joc.6219, 2020.

Hugonnet, R., McNabb, R., Berthier, E., Menounos, B., Nuth, C., Girod, L., and Kääb, A.: Accelerated global glacier mass loss in the early twenty-first century, Nature, 592, 726–731, https://doi.org/10.1038/s41586-021-03436-z, 2021.

Joughin, I.: Ice-sheet velocity mapping: A combined interferometric and speckle-tracking approach, Ann. Glaciol., 34, 195–201, https://doi.org/10.3189/172756402781817978, 2002.

Kääb, A., Winsvold, S. H., Altena, B., Nuth, C., Nagler, T., and Wuite, J.: Glacier remote sensing using Sentinel-2. Part I: Radiometric and geometric performance, and application to ice velocity, Remote Sens., 8, 598, https://doi.org/10.3390/rs8070598, 2016.

Kinnard, C., MacDonell, S., Pętlicki, M., Mendoza Martinez, C., Abermann, J., and Urrutia, R.: Mass balance and meteorological conditions at Universidad Glacier, Central Chile, in: Snow and Ice Hydrology, edited by: MacDonell, S. and Ragettli, S., CRC Press, Boca Raton, 102–123, https://doi.org/10.1201/9781315155982-5, 2018.

Masiokas, M. H., Rabatel, A., Rivera, A., Ruiz, L., Pitte, P., Ceballos, J. L., and Villalba, R.: A review of the current state and recent changes of the Andean cryosphere, Front. Earth Sci., 8, 99, https://doi.org/10.3389/feart.2020.00099, 2020.

https://doi.org/10.5194/egusphere-2026-3669
Preprint. Discussion started: 23 September 2026

Millan, R., Mouginot, J., Rabatel, A., and Morlighem, M.: Ice velocity and thickness of the world's glaciers, Nat. Geosci., 15, 124–129, https://doi.org/10.1038/s41561-021-00885-z, 2022.

Montecinos, A. and Aceituno, P.: Seasonality of the ENSO-related rainfall variability in central Chile and associated circulation anomalies, J. Climate, 16, 281–296, https://doi.org/10.1175/1520-0442(2003)016<0281:SOTERR>2.0.CO;2, 2003.

Muñoz-Sabater, J., Dutra, E., Agustí-Panareda, A., et al.: ERA5-Land: a state-of-the-art global reanalysis dataset for land applications, Earth Syst. Sci. Data, 13, 4349–4383, https://doi.org/10.5194/essd-13-4349-2021, 2021.

Nagler, T., Rott, H., Hetzenecker, M., Wuite, J., and Potin, P.: The Sentinel-1 mission: New opportunities for ice sheet observations, Remote Sens., 7, 9371–9389, https://doi.org/10.3390/rs70709371, 2015.

Paul, F., Strozzi, T., Schellenberger, T., and Kääb, A.: The 2015 surge of Hispar Glacier in the Karakoram, Remote Sens., 9, 888, https://doi.org/10.3390/rs9090888, 2017.

Podgórski, J., Pętlicki, M., Fernández, A., Urrutia, R., and Kinnard, C.: Evaluating the impact of the Central Chile Mega Drought on debris cover, broadband albedo, and surface drainage system of a Dry Andes glacier, Sci. Total Environ., 905, 166907, https://doi.org/10.1016/j.scitotenv.2023.166907, 2023.

Sánchez-Gámez, P. and Navarro, F. J.: Glacier surface velocity retrieval using D-InSAR and offset tracking techniques applied to ascending and descending passes of Sentinel-1 data for southern Ellesmere ice caps, Canadian Arctic, Remote Sens., 9, 442, https://doi.org/10.3390/rs9050442, 2017.

Schoof, C.: Ice-sheet acceleration driven by melt supply variability, Nature, 468, 803–806, https://doi.org/10.1038/nature09618, 2010.

Sole, A., Mair, D., Nienow, P., Bartholomew, I., King, M., Burke, M., and Joughin, I.: Seasonal speedup of a Greenland marine-terminating outlet glacier forced by surface melt-induced changes in subglacial hydrology, J. Geophys. Res., 116, F03014, https://doi.org/10.1029/2010JF001948, 2011.

Strozzi, T., Luckman, A., Murray, T., Wegmüller, U., and Werner, C. L.: Glacier motion estimation using SAR offset-tracking procedures, IEEE Trans. Geosci. Remote Sens., 40, 2384–2391, https://doi.org/10.1109/TGRS.2002.805079, 2002.

Vuille, M., Francou, B., Wagnon, P., Juen, I., Kaser, G., Mark, B. G., and Bradley, R. S.: Climate change and tropical Andean glaciers: Past, present and future, Earth-Sci. Rev., 89, 79–96, https://doi.org/10.1016/j.earscirev.2008.04.002, 2008.

Zemp, M., Huss, M., Thibert, E., Eckert, N., McNabb, R., Huber, J., and Cogley, J. G.: Global glacier mass changes and their contributions to sea-level rise from 1961 to 2016, Nature, 568, 382–386, https://doi.org/10.1038/s41586-019-1071-0, 2019.